



Published in final edited form as:

*Dev Cell.* 2018 March 12; 44(5): 582–596.e4. doi:10.1016/j.devcel.2018.02.010.

## PAF-Myc-Controlled Cell Stemness Is Required for Intestinal Regeneration and Tumorigenesis

Moon Jong Kim<sup>1</sup>, Bo Xia<sup>2,3</sup>, Han Na Suh<sup>1</sup>, Sung Ho Lee<sup>1</sup>, Sohee Jun<sup>1</sup>, Esther M. Lien<sup>1</sup>, Jie Zhang<sup>1</sup>, Kaifu Chen<sup>2,3</sup>, and Jae-Il Park<sup>1,4,5,6,\*</sup>

<sup>1</sup>Department of Experimental Radiation Oncology, University of Texas MD Anderson Cancer Center, Houston, Texas 77030, USA

<sup>2</sup>Center for Cardiovascular Regeneration, Houston Methodist Hospital Research Institute, Houston, Texas, USA

<sup>3</sup>Department of Cardiothoracic Surgery, Weill Cornell Medical College, Cornell University, New York, NY, USA

<sup>4</sup>Graduate School of Biomedical Sciences, University of Texas MD Anderson Cancer Center and Health Science Center, Houston, Texas 77030, USA

<sup>5</sup>Program in Genetics and Epigenetics, University of Texas MD Anderson Cancer Center, Houston, Texas 77030, USA

### SUMMARY

The underlying mechanisms how self-renewing cells are controlled in regenerating tissues and cancer remain ambiguous. PAF (PCNA-associated factor) modulates DNA repair via PCNA. Also, PAF hyperactivates Wnt/ $\beta$ -catenin signaling independently of PCNA interaction. We found that PAF is expressed in intestinal stem and progenitor cells (ISCs and IPCs) and markedly upregulated during intestinal regeneration and tumorigenesis. Whereas PAF is dispensable for intestinal homeostasis, upon radiation injury, genetic ablation of *PAF* impairs intestinal regeneration along with the severe loss of ISCs and *Myc* expression. Mechanistically, PAF conditionally occupies and transactivates *c-Myc* promoter, which induces the expansion of ISCs/IPC during intestinal regeneration. In mouse models, *PAF* knockout inhibits *Apc* inactivation-driven intestinal tumorigenesis with reduced tumor cell stemness and suppressed Wnt/ $\beta$ -catenin signaling activity,

\*Correspondence: jaeil@mdanderson.org.

<sup>6</sup>Lead Contact

### AUTHOR CONTRIBUTIONS

M.J.K. and J.-I.P. conceived the experiments; M.J.K., H.N.S., S.H.L., S.J., E.M.L., and J.Z. performed the experiments; B.X. and K.C. analyzed RNA-Seq results; M.J.K. and J.-I.P. analyzed the data; M.J.K. and J.-I.P. wrote the manuscript.

### DECLARATION OF INTERESTS

The authors declare no competing interests.

### Supplemental Tables

Table S1. List of PAF up- and down-regulated signaling identified by KEGG analysis (Related to Figure 7 and Figure S7)

Table S2. Result of GSEA analysis of *PAF*KO cells (Related to Figure 7 and Figure S7)

**Publisher's Disclaimer:** This is a PDF file of an unedited manuscript that has been accepted for publication. As a service to our customers we are providing this early version of the manuscript. The manuscript will undergo copyediting, typesetting, and review of the resulting proof before it is published in its final citable form. Please note that during the production process errors may be discovered which could affect the content, and all legal disclaimers that apply to the journal pertain.

supported by transcriptome profiling. Collectively, our results unveil that PAF-Myc signaling axis is indispensable for intestinal regeneration and tumorigenesis by positively regulating self-renewing cells.

## eTOC Blurp

Controlling the proliferation of self-renewing cells is crucial for tissue homeostasis and regeneration. Kim et al. show that PAF (PCNA-associated factor), dispensable for intestinal homeostasis, is required to positively regulate the proliferation of self-renewing cells via *Myc* transactivation during intestinal regeneration and tumorigenesis.

## Keywords

PAF; Myc; intestinal regeneration; stem/progenitor cells; intestinal stem cells; colorectal cancer; cancer stem cells; Wnt signaling;  $\beta$ -catenin

## INTRODUCTION

Stem cells play key roles in tissue homeostasis and regeneration by self-renewing and repopulating progenitor cells (Fuchs et al., 2004; Morrison and Spradling, 2008). In the small intestine, two major ISCs co-exist. Crypt base columnar cells (CBC) ISCs marked by the high *Lgr5* expression are highly proliferative and essential for the intestinal homeostasis (Barker et al., 2007). The other ISCs located at position 4 (+4) and labeled by *Hopx*, *Lgr1*, *Bmi1*, and *Tert* are quiescent during intestinal homeostasis, whereas conditionally activated upon tissue damage. (Montgomery et al., 2011; Powell et al., 2012; Sangiorgi and Capecchi, 2008; Takeda et al., 2011). Accumulating evidence suggests that +4 ISCs function as a reservoir of ISCs during regeneration (Buczacki et al., 2013; Tian et al., 2011). Additionally, the committed progenitor cells (*Dll1*<sup>+</sup>, *Alpi*<sup>+</sup>, and *Krt19*<sup>+</sup>) located above the position +4 cells also dedifferentiate into ISCs for intestinal regeneration (Asfaha et al., 2015; Tetteh et al., 2016; Van Es et al., 2012), implying the involvement of the cell plasticity in rebuilding intestinal epithelium. Although the extensive lineage tracing studies have been used to identify ISCs or reservoir ISCs/IPC populations, still the underlying mechanisms how these ISCs/IPC cells are activated and expanded during regeneration remain elusive.

It was proposed that cancer stem cells (CSCs) are a subpopulation of tumor cells, which drives tumor growth by self-renewing and giving rise to the daughter cells (Nguyen et al., 2012). The identities of CSCs are still controversial, however, it is plausible that CSCs might be related to therapeutic resistance and tumor recurrence (Dean et al., 2005; Kreso and Dick, 2014). Expression of *CD44*, *CD133*, and *Lgr5* have been suggested as a maker for stemness of colorectal cancer (CRC) cells (O'Brien et al., 2007; Ricci-Vitiani et al., 2007; Schepers et al., 2012; Zeilstra et al., 2008; Zhu et al., 2009). Nonetheless, how CSCs are maintained and expanded were not fully understood.

PAF (also known as *p15/KIAA0101/NS5ATP9/OEACT-1*) was initially identified as a proliferating cell nuclear antigen (PCNA)-interacting protein (Yu et al., 2001). PAF is implicated in both DNA repair and cell proliferation (Emanuele et al., 2011; Povlsen et al.,

2012). PAF binds to PCNA sliding clamp and regulates DNA replication and repair (De Biasio et al., 2015). Importantly, *PAF* expression is significantly upregulated in many human cancers (Cheng et al., 2013; Hosokawa et al., 2007; Jain et al., 2011; Jung et al., 2013; Kais et al., 2011; Kato et al., 2012; Mizutani et al., 2005; Wang et al., 2016; Yu et al., 2001; Yuan et al., 2007). In pancreatic cancer cells, *PAF* overexpression is necessary for pancreatic cancer cell proliferation (Hosokawa et al., 2007). Additionally, PAF is associated with MAPK hyperactivation *via* transcriptional activation of the late endosomal/lysosomal adaptor, MAPK and mTOR activator 3 (*LAMTOR3*), which is involved in the initiation of pancreatic intraepithelial neoplasia (Jun et al., 2013). Moreover, PAF hyperactivates Wnt/ $\beta$ -catenin signaling in CRC cells as a co-factor of  $\beta$ -catenin/EZH2 transcriptional complex, resulting in the development of intestinal adenoma (Jung et al., 2013).

In this study, we sought to interrogate how stem cells are activated by radiation injury. Our unbiased gene expression screening identified that, among DNA repair-related genes, *PAF* expression is associated with controlling ISCs/IPC. Further comprehensive and genetic approaches revealed that PAF-Myc signaling axis is indispensable for intestinal regeneration and tumorigenesis by positively controlling the expansion of stem cells.

## RESULTS

### Upregulation of *PAF* Expression upon Radiation Injury

To identify essential genes associated with DNA repair during tissue regeneration, we conducted qRT-PCR array for DNA repair gene collections from irradiation (IR) treated mouse small intestine (1 day post-injury [1 dpi], 10 Gy) (Figures 1A and 1B). Among differentially expressed 79 genes, *PAF* expression was highly upregulated by IR (7<sup>th</sup> ranked). Additionally, IR upregulated *PAF* expression in the mouse small intestine in a dose- and time-dependent manner (Figures 1C and 1D), which led us to hypothesize that PAF plays crucial roles in intestinal regeneration.

### PAF Expression in Replenishing and Regenerating Intestinal Crypts

To elucidate the *in vivo* roles of PAF in intestinal regeneration, we generated *PAF*KO mouse model using clustered regularly interspaced short palindromic repeat (CRISPR)/Cas9 gene targeting system (Wang et al., 2013; Yang et al., 2013)(Figure S1). Of note, *PAF*KO mice are viable without any discernible phenotypes. To examine PAF expression in the crypt, we conducted immunohistochemistry (IHC) using two different PAF monoclonal antibodies (Figures 2A and S2B). We confirmed the specificity of PAF antibody using *PAF*KO mice as a negative control (Figures 2A and S2B). We located 5~10 cells of PAF positive (PAF+) cells existed in the one section of crypt (Figures 2A and 2B). PAF was expressed in 1~2 cells of CBC ISCs and 3~8 cells of transit-amplifying (TA) cells (Figures 2A and 2B), but not in the villi (Figure S2A). Most PAF+ cells belong to Ki67+ cells (17.71% of Ki67+ cells), a marker for cell proliferation (Figures 2C and 2E). Despite the additional role of PAF in DNA repair as a PCNA-interacting protein (Povlsen et al., 2012), only 23.01% of PAF+ cells were PCNA+ cells (Figures 2D and 2E). Furthermore, *PAF*KO mice did not display differences in the expression of *PCNA* in the crypts, compared to *PAF*wild-type (WT) mice (Figure 2F), implying the existence of PCNA-independent functions of PAF in the intestine.

To determine whether PAF is expressed in ISCs, we used a *Lgr5-EGFP-CreERT* knock-in mouse. PAF<sup>+</sup> cells were correlated with Lgr5<sup>+</sup> CBC cells and Lgr5<sup>+</sup> progenitor cells localized at transit amplifying zone (TA zone) (Figure 2H), confirmed by qRT-PCR of fluorescence-activated cell sorting (FACS)-isolated Lgr5<sup>+</sup> cells (Figure 2I). The Paneth cells between CBC ISCs did not express PAF (Figure 2G). We further asked whether PAF is expressed in the quiescent ISCs at position 4, using *TERT-tdTomato-CreERT2* (Jun et al., 2016) and *Bmi1-EGFP* (Hosen et al., 2007) knock-in mice. Some population of TERT<sup>+</sup> (52.94%) and Bmi1<sup>+</sup> cells (63.16%) expressed PAF (Figures 2J, 2K, S2D, and S2E). These results indicate that PAF<sup>+</sup> cells include some population of CBC (Lgr5<sup>high</sup>) ISCs, position 4+ ISCs (TERT<sup>+</sup> and Bmi1<sup>+</sup>), and TA progenitor (Lgr5<sup>low</sup>) cells.

Given the upregulation of *PAF* expression by IR (Figure 1), we monitored PAF<sup>+</sup> cells in the regenerating intestinal crypts. Interestingly, upon IR exposure (10 Gy), the number of PAF<sup>+</sup> cell was increased until 4 dpi and then decreased at 7 dpi (Figures 2L and 2M), which is consistent with *PAF* mRNA upregulation (Figures 1C and 1D). At 1~2 dpi, the remaining ISCs started to divide. At 4 dpi, the regenerating crypts were enlarged, and newly generating CBC cells and TA cells reappeared. At 7 dpi, the regeneration process was mostly completed (Jun et al., 2016; Suh et al., 2017). Intriguingly, PAF<sup>+</sup> cells remained at position 4-6 and 8-9 at 1~2 dpi, whereas PAF<sup>+</sup> CBC cells were lost by cell death at 1 dpi (Figures 2L and 2M). The newly generated CBC cells and TA cells highly expressed PAF at 4 dpi, and PAF<sup>+</sup> cells were partially restored as CBC and TA cells (7 dpi) (Figures 2L and 2M). Given the high enrichment of PAF expression in the remaining and active ISCs/IPCs in the regenerating crypts, these results imply that PAF might be involved in controlling ISCs/IPCs during regeneration.

### Impaired Intestinal Regeneration by *PAF* KO

To directly test whether PAF is engaged in intestinal regeneration, we utilized *PAF* KO mouse model. Prior to the experiments, we examined the intestinal morphology and several differentiated intestinal epithelial cell (IEC) markers in *PAF* KO mice. *PAF* KO mice displayed no differences in intestinal morphology and IEC differentiation (Figures S3A and S3B). To further address whether *PAF* KO affects intestinal homeostasis, we performed BrdU incorporation assays (Figures S3C and S3D). The number of BrdU incorporated cells in the crypts of *PAF* KO mice was the same as that in WT after 2h BrdU induction (Figure S3C). Furthermore, *PAF* KO mice showed a similar migration rate during 3 days of tracing of BrdU<sup>+</sup> cells (Figure S3D). These data indicate that genetic ablation of *PAF* does not affect the proliferation and migration of IECs. Additionally, we analyzed the expression of various genes related to intestinal homeostasis by qRT-PCR (Figure S3E). Despite the slight decrease of *c-Myc* expression in *PAF* KO intestine (~36%), the expression of most genes was not altered in the crypts of WT and *PAF* KO mice. It is noteworthy that conditional deletion of *c-Myc* in the intestine has no impact on intestinal homeostasis (Bettess et al., 2005). These results suggest that PAF is dispensable for intestinal homeostasis.

Next, we asked whether PAF is required for tissue regeneration. We found that upon IR injury, *PAF* KO mice showed severe defects in the intestinal regeneration (Figures 3A-3D). At 4 dpi, the number of viable crypts was markedly reduced by 10 Gy (50.5% decrease) and

12 Gy (100% decrease) IR treatment (Figures 3B and 3E). The crypt structure, represented by lysozyme staining, was also severely disintegrated in *PAFKO* mice (Figures 3D and 3F) compared to that in WT mice. These results suggest that PAF is indispensable for intestinal regeneration.

### PAF Is Required for ISCs/IPC Expansion in Regenerating Crypts

To understand the underlying mechanism of intestinal regeneration defects by *PAFKO*, we first examined DNA repair process in *PAFKO* mice. Interestingly, no significant increase of cell death (Apoptotic body and Active-Caspase 3 staining) was detected in *PAFKO* mice during 48h after IR (Figures S4A-S4D). Initial recognition of DNA damages, checked by ATM pS1981(1h) and phospho- $\gamma$ H2AX (6h) (Figures S4E, S4F, and S4G), and downstream targets of DNA damage responses were not changed in *PAFKO* mice (Figures S4H-S4K). DNA double-strand breaks repair (6h~48h after IR) represented by  $\gamma$ -H2AX was also similar between *PAF*WT and KO mouse intestine samples (Figures S4E and S4F). These data suggest that regeneration defects in *PAFKO* mice are not due to impaired DNA repair processes.

Next, given the specific expression of PAF in ISCs/IPC (Figures 2H-2K), we asked whether *PAFKO*-induced defects in intestinal regeneration is due to the dysfunction of ISCs/IPC. To test this, we performed crypt organoid culture assays. Interestingly, the crypt organoids derived from *PAFKO* mice showed the low efficiency of organoid formation (Figures 4A and 4B) as well as decreased growth and budding efficiency (Figures 4A, 4C, and 4D). These results imply that PAF might be required for intestinal regeneration possibly by controlling ISCs/IPC in a cell-autonomous manner.

To further assess underlying mechanisms of dysregulated ISCs/IPC in *PAFKO* mice during intestinal regeneration, we generated *PAFKO;Lgr5-EGFP-CreERT* mice and analyzed the *Lgr5*<sup>+</sup> ISCs/IPC population after radiation injury. After IR treatment, *Lgr5*<sup>high</sup> ISCs cells are depleted by DNA damage-induced apoptosis. However, a small population of *Lgr5*<sup>low</sup> cells (including quiescent ISCs and TA progenitor cells) survives and contributes to intestinal regeneration (Buczacki et al., 2013; Metcalfe et al., 2014; Muñoz et al., 2012). In the normal intestine of *PAFKO* mice, the number of *Lgr5*<sup>+</sup> ISCs/IPC was not changed (Figures S5A and S5B), which is consistent with the BrdU incorporation assay results (Figures S3C and S3D). Similarly, *PAFKO* did not affect the number of *Lgr5*<sup>low</sup> cells population upon IR (Figures S5C and S5D), suggesting *PAFKO* has no effects on *Lgr5*<sup>+</sup> ISCs/IPC on the overall cell viability in the early stage of regeneration (1 dpi, 10 Gy). However, *PAFKO* mice exhibited significantly delayed restoring the *Lgr5*<sup>+</sup> cells in regenerating crypts at the late time point (7 dpi) (Figures 4E-4H). Of note, in the treatment of 10 Gy IR, *PAFKO* mice displayed about 50% of viable crypts (4 dpi) (see Figures 3A-3E). Although the regenerating crypts restored their morphology similar to WT in *PAFKO* mice (7 dpi), the number of *Lgr5*<sup>+</sup> cells were not restored. To complement the *in vivo* result of *PAFKO*-decreased *Lgr5*<sup>+</sup> ISCs/IPC, we also employed single cell organoid cultures of FACS-isolated *Lgr5*<sup>+</sup> cells from the mouse intestine. Strikingly, single cell organoids from *PAFKO* *Lgr5*<sup>+</sup> cells showed three times lower efficiency in the organoid formation and displayed severe growth defects compared to *PAF*WT *Lgr5*<sup>+</sup> organoids

(Figures 4I-4K). *PAFKO* Lgr5<sup>+</sup> cells grew markedly slowly during the 2 weeks in single cell organoid culture. These *in vivo* and *in vitro* results suggest that PAF is required for the expansion of ISCs/IPC during intestinal regeneration.

### PAF Transactivated *c-Myc* Is Required for ISCs/IPCs Expansion upon Radiation Injury

Next, we sought to determine the molecular mechanism of PAF-induced ISCs/IPC expansion. We collected remaining Lgr5<sup>+</sup> cells from IR-treated intestine samples of *Lgr5-EGFP-CreERT* and *PAFKO* mice and examined the expression of target genes of the Wnt, Notch, Hippo-YAP, Hedgehog, and TGF- $\beta$ /BMP pathways (Figure 4L and S5E). In the regenerating crypts (1 and 2 dpi), remaining Lgr5<sup>low</sup> cells from *PAFKO* mice exhibited a marked decreased expression of Wnt target genes (*c-Myc*, *Cyclin D1*, and *Lgr5*) (Figure 4L and S5E). The well-established Wnt target gene, *Axin2*, was also decreased in the remaining Lgr5<sup>low</sup> cells at 2 dpi. Downregulation of Wnt target genes was also observed in whole crypts fraction at the late time point (4 dpi) (Figure S5F). IHC confirmed that *c-Myc* and *Cyclin D1* expression was significantly downregulated in 4 dpi *PAFKO* mouse intestine (Figures 5A, 5B, and S5G-S5I). Additionally, we found notable PAF<sup>+</sup>:Myc<sup>+</sup> cells in position 4-6 at 1 dpi, when ISCs are activated for repopulation (Figure 5C). Whereas *c-Myc* expression was upregulated during regeneration, *PAFKO* showed a decrease in *c-Myc* expression (Figures S5G-S5I). These results suggest that PAF might be required for *c-Myc* upregulation during intestinal regeneration.

As a cofactor of  $\beta$ -catenin transcription complex, PAF upregulates *c-Myc* expression in CRC (Jung et al., 2013), which led us to determine whether PAF transactivates *c-Myc* in the regenerating intestine. To test this, we performed a chromatin immunoprecipitation (ChIP) assay of the mouse small intestine using PAF antibody. The small intestine samples from *PAFKO* mice served as a negative control (Figure 5D; Lane 4). We found that endogenous PAF occupied the TCF-binding element (TBE)-containing proximal promoter of *c-Myc* and *CCND1* (*Cyclin D1*) in the normal intestine (Figure 5D; Lane 1, 0 dpi). It is noteworthy that despite the massive death of PAF<sup>+</sup> cells upon IR, some PAF<sup>+</sup> cells survived at 1 dpi (Figures 2L and 2M). Nonetheless, we found that IR conditionally induced the recruitment of PAF and  $\beta$ -catenin to the *c-Myc* promoter (Figure 5D; lane 3, 2 dpi). These results suggest that PAF is conditionally associated with and transactivates the *c-Myc* promoter during intestinal regeneration, similar to PAF-induced *c-Myc* transactivation in CRC cells (Jung et al., 2013).

Next, we asked whether *c-Myc* mediates PAF-controlled ISCs/IPC expansion by rescue assay of the Lgr5<sup>+</sup> single cell organoid culture. We found that ectopic expression of *c-Myc* using retrovirus rescued the reduction of organoid-forming efficiency and proliferation in *PAFKO* Lgr5<sup>+</sup> organoids (Figures 5E-5G). These results suggest that PAF-transactivated *c-Myc* is required for ISCs/IPC expansion during intestinal regeneration.

Additionally, we performed rescue experiments using wild-type PAF and PIP mutant PAF (mutPIP-PAF) (Jung et al., 2013). It has been suggested that the function of PAF in DNA repair is mediated by the interaction of PAF with PCNA *via* PIP, a PCNA-interacting protein motif (Emanuele et al., 2011; Povlsen et al., 2012). However, mutPIP-PAF expression was sufficient to recover *PAFKO* single cell organoids (Figures 5H and 5I), suggesting that PAF-



mediated DNA repair through PCNA binding is not involved in growth defect of *PAFKO* organoids.

### Attenuation of Intestinal Tumorigenesis by *PAFKO*

PAF is significantly upregulated in many human cancers (Cheng et al., 2013; Hosokawa et al., 2007; Jain et al., 2011; Jun et al., 2013; Jung et al., 2013; Kais et al., 2011; Kato et al., 2012; Mizutani et al., 2005; Wang et al., 2016; Yu et al., 2001; Yuan et al., 2007), indicating the potential roles of PAF in promoting tumorigenesis. Additionally, given the pivotal roles of PAF and c-Myc in controlling ISCs/IPC's activation (Figures 5 and S5G-S5I) and initiating intestinal tumorigenesis (Jung et al., 2013; Sansom et al., 2007), we next asked whether PAF contributes to intestinal tumorigenesis by positively modulating the cancer cell stemness. We assessed the expression of *PAF* in intestinal adenomas driven by *Apc* mutation using *Apc*<sup>Min/+</sup> mouse model (Moser et al., 1990). IHC results showed that PAF was markedly upregulated in intestinal adenomas of *Apc*<sup>Min/+</sup> mice (Figure 6A). sqRT-PCR of individually isolated intestinal adenomas and adjacent normal intestine samples of *Apc*<sup>Min/+</sup> mice (age of 14 and 16 weeks) also showed the marked upregulation of *PAF* in *Apc* mutation-driven adenomas (Figure 6B), which confirms the upregulation of PAF in CRC (Jung et al., 2013). Of note, PAF<sup>+</sup> cells were a subpopulation of Ki67<sup>+</sup> or PCNA<sup>+</sup> cells in adenomas (27.68% and 26.49%, respectively)(Figures S6A-S6D).

To test whether genetic ablation of *PAF* suppresses tumorigenesis in a mouse model, we established *Apc*<sup>Min/+</sup> (control group) and *PAFKO;Apc*<sup>Min/+</sup> compound strains (experimental group) and. The median survival of *Apc*<sup>Min/+</sup> mice was 117 days (N=16). Surprisingly, *PAFKO;Apc*<sup>Min/+</sup> mice displayed marked extended survival (median 184 days, N=17; P=0.0001) (Figure 6C). Moreover, *PAFKO;Apc*<sup>Min/+</sup> mice showed a decreased number and size of adenomas, compared to those in *Apc*<sup>Min/+</sup> mice (Figures 6D, 6F, and S6E). Of note, *PAF* heterozygous KO (*PAFHet;Apc*<sup>Min/+</sup>) did not affect mouse survival and the number and size of adenomas compared to *PAFKO;Apc*<sup>Min/+</sup> (Figures 6C-6F). Ki67 IHC showed reduced cell proliferation in adenomas developed in *PAFKO;Apc*<sup>Min/+</sup> mice compared to that in *Apc*<sup>Min/+</sup> control mice (Figures 6G and 6H). The number of Paneth cells was also diminished in intestinal adenomas of *PAFKO;Apc*<sup>Min/+</sup> mice (Figures 6I and 6J). Given that the Paneth cell differentiation is driven by Wnt/ $\beta$ -catenin signaling (van Es et al., 2005), it is possible that *PAFKO* might induce the overall downregulation of Wnt/ $\beta$ -catenin target genes in tumor cells. Based on our previous finding that PAF hyperactivates the Wnt signaling as a cofactor of the  $\beta$ -catenin transcriptional complex (Jung et al., 2013), we tested whether *PAFKO* suppresses Wnt/ $\beta$ -catenin signaling in intestinal adenomas. While *PAFKO* did not affect the level and activity of the  $\beta$ -catenin protein in adenomas (Figures 6K and 6L), *PAFKO* notably downregulated the expression of Wnt/ $\beta$ -catenin target genes, c-Myc and Cyclin D1, in intestinal adenomas (Figures 6M-6O and S6G). Furthermore, we found that PAF was co-expressed with c-Myc in intestinal adenomas of *Apc*<sup>Min/+</sup> mice, similar to their co-expression in the regenerating crypts (Figure 6N and S6F). These results suggest that *PAFKO* attenuates intestinal tumorigenesis by downregulation of  $\beta$ -catenin target genes including c-Myc.

## Reduced CRC cell stemness by PAF KO

Previously, we found that PAF-Wnt signaling axis is required for the maintenance of breast cancer cell stemness (Wang et al., 2016). Moreover, having determined that PAF is indispensable for ISC/IPC expansion in regeneration (Figures 4), we next examined the role of PAF in controlling the stemness of CRC cells. We analyzed the expression of several known CRC stemness makers (CD44, CD133, and Lgr5) (O'Brien et al., 2007; Ricci-Vitiani et al., 2007; Schepers et al., 2012; Zeilstra et al., 2008; Zhu et al., 2009). Adenomas from *PAFKO;Apc<sup>Min/+</sup>* mice showed marked decreased expression of CRC stemness markers (CD44, CD133, and Lgr5)(Figures 7A-7D, S7A, and S7B). To better understand the role of PAF in CRC cell stemness, we cultured tumor organoids from *Apc<sup>Min/+</sup>* and *PAFKO;Apc<sup>Min/+</sup>* crypts. Owing to hyperactivation of Wnt signaling, *Apc<sup>Min/+</sup>* organoids develop into the sphere shape (cystic) without budding (Sato et al., 2011a). Surprisingly, the organoids derived from *PAFKO;Apc<sup>Min/+</sup>* mouse intestine showed severe defects in growth (Figures 7E and 7F). Although the initial organoid forming efficiency was similar (Figure 7G), *PAFKO;Apc<sup>Min/+</sup>* organoids did not grow until 21 days, compared to the organoids from *PAFWT;Apc<sup>Min/+</sup>* (Figures 7E and 7F). One copy deletion of PAF (*PAFHet;Apc<sup>Min/+</sup>*) did not suppress the cystic organoid growth (Figure S7C), consistent with *in vivo* results from *PAFHet;Apc<sup>Min/+</sup>* mice (see Figures 6C-6F). We further assessed the effects of PAF knockdown on cancer cell stemness using human CRC cells. Colorectal CSCs exhibit the enrichment of CD44 and CD133 expression (Kemper et al., 2010; O'Brien et al., 2007; Ricci-Vitiani et al., 2007). We found the significantly decreased population of CD44<sup>+</sup>:CD133<sup>+</sup> cells in PAF-depleted HT29 cells (Figure S7D). Furthermore, PAF knockdown inhibited colonosphere formation of HT29 (Figure S7E and S7F). These results suggest that PAF is required for the maintenance of CRC cell stemness.

Next, for an unbiased assessment of PAF-controlled transcriptome in intestinal tumors, we also performed RNA-seq of *PAFWT* and *KO Apc<sup>Min</sup>* mouse tumors (Figure 7H). Kyoto Encyclopedia of Genes and Genomes (KEGG) analysis showed that Wnt signaling is markedly downregulated in *PAFKO* tumor cells (Figures 7I, S7G, and Table S1), which was also confirmed by Gene Set Enrichment Analysis (GSEA) (Figure 7J and Table S2). These results strongly suggest that PAF positively modulates Wnt/ $\beta$ -catenin signaling in CRC, similar to that during intestinal regeneration.

## DISCUSSION

Herein, our comprehensive approaches revealed that the PAF-Myc axis is required for ISC/IPC expansion during intestinal regeneration and tumorigenesis.

c-Myc is not required for normal intestine homeostasis but is indispensable for intestinal regeneration (Ashton et al., 2010; Bettess et al., 2005). However, it was unknown how c-Myc contributes to intestinal regeneration. In our experimental setting, ectopic expression of c-Myc rescued *PAFKO*-induced defects in Lgr5<sup>+</sup> single cell organoid growth (see Figures 5E-5G), which strongly suggests that c-Myc mediates PAF-controlled ISC/IPC expansion during intestinal regeneration. Interestingly, *PAFKO* did not affect intestinal homeostasis, which requires constitutively active Wnt signaling in the crypts. Nonetheless, there were no changes in the expression of Wnt/ $\beta$ -catenin target genes (*Cyclin D1*, *CD44*, and *Lgr5*) in



*PAFKO* intestine (without IR injury)(see Figure S3E). However, under specific physiologic or pathologic conditions such as regeneration or tumorigenesis when enhanced Wnt signaling is required (Cadigan and Waterman, 2012; Clevers and Nusse, 2012; Polakis, 2012), the highly upregulated PAF hyperactivates Wnt/ $\beta$ -catenin transcriptional complex and transactivates *c-Myc*, which subsequently triggers the activation of self-renewing cells (Figures 5J and 7K). This is also supported by the marked upregulation of PAF expression in the regenerating crypts (see Figures 1A-1C, and 2L) and CRC (Jung et al., 2013).

Accumulating evidence suggests the pivotal roles of *c-Myc* in regulating stem cells. *c-Myc* is necessary for efficient cellular reprogramming of induced pluripotent stem cells (iPSCs) (Araki et al., 2011; Takahashi et al., 2007). In ESCs, *c-Myc* modulates cell stemness and differentiation by amplifying protein biosynthesis (Nie et al., 2012; Varlakhanova et al., 2010). *c-Myc* also regulates the balance between self-renewing and differentiated/committed hematopoietic stem cells by controlling the interaction with their niche (Laurenti et al., 2008; Wilson et al., 2004). Given the specific and dynamic expression of PAF in ISCs/IPC cells (see Figures 2) and PAF-transactivated *c-Myc* (see Figure 5), it is probable that PAF may play pivotal roles in governing various stem cells *via c-Myc*. Indeed, in the small intestine, *PAFKO* decreased the expression of stem cell marker, *Lgr5*, in the regenerating crypts accompanied with the downregulation of *c-Myc*. Furthermore, *c-Myc* rescued *PAFKO*-induced failure of organoid growth (see Figures 5E-5G), indicating that PAF functions as an upstream molecule of *c-Myc* in controlling the stem cells.

70% of human CRC displays a significant upregulation of *c-Myc* (Erisman et al., 1985; Sikora et al., 1987). In mouse models, genetic ablation of *c-Myc* suppresses intestinal tumorigenesis driven by *Apc* mutations (Sansom et al., 2007). Similarly, *PAFKO* inhibits intestinal adenoma development in *Apc<sup>Min/+</sup>* mice with reduced *c-Myc* expression (see Figures 6M and S6G). Moreover, the depletion of *PAF* decreased the expression of CRC cell stemness markers, (CD44, CD133, and *Lgr5*) in *Apc<sup>Min</sup>* adenomas (see Figures 7A-7D) with downregulation of *c-Myc* (see Figures 6M and 7A). Although the effects of *PAFKO* on CRC cell stemness should be further elaborated with cell ablation, lineage-tracing, and serial transplantation assays, our results are somewhat similar to our previous study that PAF is required for the maintenance of breast cancer cell stemness (Wang et al., 2016). Although *Myc* depletion rescued phenotypes of tumorigenesis driven by *APC* mutation in the mouse model (Sansom et al., 2007), the ectopic expression of *Myc* failed to rescue the organoid growth in *PAFKO;Apc<sup>Min/+</sup>* condition. These results imply that additional factors/pathways might be involved in PAF-controlled CRC cell stemness. Transcriptomic analysis of *Apc<sup>Min/+</sup>* and *PAFKO;Apc<sup>Min/+</sup>* adenomas revealed that in addition to Wnt signaling, other oncogenic pathways including Hedgehog and TGF-G signaling were modulated by PAF (Figures 7H-7J and S7H). Given the oncogenic function of Hedgehog and TGF-G signaling in CRC (Munoz et al., 2006; Takaku et al., 1998; Varnat et al., 2009), it is possible that PAF-controlled colorectal cancer stemness is mediated by several oncogenic pathways including Wnt-Myc, Hedgehog, and TGF- $\beta$  signaling. Although we here limited our scope to PAF-activated Wnt-Myc axis, it is necessary to further examine how PAF is associated with various oncogenic signalings beyond Wnt/ $\beta$ -catenin pathway.

PAF directly binds to PCNA (De Biasio et al., 2015). Nonetheless, it is highly likely that PAF-controlled stem cells might be independent of PCNA interaction, which is supported by the following results: (a) Without IR treatment, *PAF* KO is sufficient to suppress organoid growth (Figures 4A-4D and 4I-4K), which rules out the potential involvement of PAF-mediated DNA repair in tissue regeneration; (b) PAF transactivates  $\beta$ -catenin target genes including *c-Myc* in a PCNA-independent manner (Jung et al., 2013); (c) Instead of DNA repair genes, *c-Myc* is sufficient to rescue the *PAF* KO phenotypes in the single cell organoid growth (see Figures 5E-5G); (d) Ectopic expression of PIP-mutated PAF fully rescues the defect of *PAF* KO organoid growth (see Figures 5H and 5I); (e) Only some of PCNA<sup>+</sup> cells are PAF<sup>+</sup> cells in the normal intestine (26.49%) and adenomas (23.01%) (see Figures 2D, 2E, S6C, and S6D), indicating the potential roles PAF in a PCNA-independent manner; (f) *PAF* KO mice showed no abnormality in PCNA expression and IECs growth in the crypts (see Figure 2F); (g) *PAF* KO did not affect the DNA double-strand breaks and DNA damage foci formation in the intestine (see Figures S4E and S4F), indicating that PAF is dispensable for genomic stability or DNA repair. Thus, these results strongly support that PAF-mediated intestinal regeneration is independent of PCNA and DNA repair pathway.

Although PAF<sup>+</sup> cells partially mark ISC and TA cells in the normal intestine, *PAF* KO mice did not display defects in tissue homeostasis (see Figures S3). Tissue injury upregulates PAF expression, which enhances *c-Myc* transcription for the subsequent expansion of ISCs/IPCs. This is also supported by co-expression of PAF and *c-Myc* in the surviving cells (not the Paneth cells) of regenerating crypts (see Figure 5C). Employing PAF reporter and lineage tracing mice will provide further insights into how PAF<sup>+</sup> cells contribute to tissue regeneration and cancer.

Despite the crucial roles of PAF in regulating self-renewing cells in intestinal regeneration and tumorigenesis, it is still unclear how PAF is upregulated in the regenerating crypts and CRC. Due to the high expression of PAF in *Apc*<sup>Min/+</sup> tumors (see Figures 6A and 6B), it is reasonable that Wnt/ $\beta$ -catenin signaling might directly transactivate *PAF*. Although the proximal promoter of *PAF* contains multiple TBEs (Wang et al., 2016), we found that manipulation of Wnt/ $\beta$ -catenin signaling did not affect the transcription of *PAF* in both IECs and CRC cells (Figures S7I and S7J). Given our previous finding that Oct4, Nanog, and Sox2 transactivate *PAF* in breast cancer cells and mammary epithelial cells (Wang et al., 2016), the involvement of such iPSC-inducing factors in PAF regulation should be addressed in future studies.

PAF is significantly upregulated in CRC and contributes to tumorigenesis, whereas dispensable for tissue homeostasis. Therefore, PAF might be a viable molecular target for cancer treatment with minimal damage to the normal cells. Conversely, tweaking PAF might provide new ways to manipulate tissue regeneration. Collectively, our findings unveil the essential role of the PAF-Myc signaling axis in controlling stem cell activation in regeneration and cancer.

## STAR METHODS

### CONTACT FOR REAGENT AND RESOURCES SHARING

Additional information and requests for reagents should be directed to and will be fulfilled by the Lead Contact, Jae-Il Park at jaeil@mdanderson.org

### EXPERIMENTAL MODEL AND SUBJECT DETAILS

**Mouse Strains**—We generated *PAF* KO strain using CRISPR/Cas9 gene targeting system. *Apc<sup>Min/+</sup>* (JAX: 002020) and *Lgr5-EGFP-IRES-CreERT2* (JAX: 008875) mice were obtained from the Jackson Laboratory. All mice were maintained on a C57BL/6 background except *Bmi1<sup>EGFP</sup>* mice (BKa.Cg-*Ptprcb Bmi1<sup>tm1llwThy1a/J</sup>*). Both male and female of *PAF* KO, C57BL/6J (WT control), or *Lgr5-EGFP* compound strains were used for regeneration experiments in 8-10 weeks of age. For intestinal adenoma quantification and Kaplan-Meier survival curve, only male mice (*Apc<sup>Min/+</sup>* and *PAF* KO; *Apc<sup>Min/+</sup>* compound strains) were used. All mouse experiments were performed under MD Anderson guidelines and Association for Assessment and Accreditation of Laboratory Animal Care International standards.

### METHOD DETAILS

**Generation of *PAF* KO Mice**—To establish *PAF* KO mice, two guide RNAs (gRNAs) targeting exon 1 of *PAF* gene and Cas9 mRNA (Sigma) were injected into the mouse zygotes (The Genetically Engineered Mouse Facility, MD Anderson). gRNA sequences were as follows: #1: 5'-GTTCCCGCCACCGTTTAAATGGG-3', #2: 5'-ACCAAAGCAAACACTACGTTCCAGG-3'. Four strains harboring *PAF* mutation (gene targeting efficiency: 4/7=57.14%) were identified. Two heterozygote strains (strain 4 and 7) carrying 118bp and 125bp deletion of *PAF* (*PAF null*) between the two gRNAs targeted region were selected as founders. Using the strain 7 as a founder, at least 5 times subsequent backcross with C57BL/6 was conducted to minimize the off-target effects. For PCR genotyping of *PAF* KO following primer pairs and cycling conditions were used: primers: #F: 5' - AGAATCGAGGTTCTCAAGCG-3'; #R: 5' - CCTTCTAGCTGCTCAATGGG-3', PCR conditions: 10 min at 95°C, followed by 40 cycles of 95°C for 15 sec, 65°C for 15 sec, 72°C for 30 sec and post-elongation at 72°C for 5 min. *PAF* WT makes 280 bp, and *PAF* KO makes 155bp (125bp deletion) of PCR product.

**Radiation Injury**—For intestinal damage, 8-10 weeks old mice were treated with  $\gamma$ -irradiation (10 or 12 Gy) using irradiator (Nasatron). The intestinal regeneration was assessed at 4 and 7 dpi.

**Gene Expression Analysis**—For small-scale screening of DNA repair gene expression in mice, mRNAs from the irradiated mouse small intestines (1 dpi, 10 Gy) were analyzed with RT<sup>2</sup> Profiler™ PCR Array Mouse DNA Repair (Qiagen). Control and experimental mice were used for analysis (N=3, each). RNA was extracted from the mouse small intestine and organoids using the TRIzol (Invitrogen) as the manufacturer's instructions. iScript cDNA synthesis kit (Biorad) with 1  $\mu$ g of RNA was used for cDNA synthesis. For gene expression analysis of *Lgr5*+ cells, sorted 100-500 *Lgr5*+ cells were collected from

*Lgr5<sup>EGFP</sup>* or *PAFKO;Lgr5-EGFP* mice in normal and IR-treated conditions. cDNA was synthesized using REPLI-g WTA Single Cell Kit (Qiagen #150063). The quantitative real-time PCR (qRT-PCR) was performed using a 7500 real-time PCR machine (Applied Biosystems) with specific primers listed in Table S3. Target gene expression was normalized by Hypoxanthine phosphoribosyltransferase 1 (*HPRT1*) or *18s* rRNA. Comparative  $2^{-Ct}$  methods were used for quantification of qRT-PCR results.

**Crypt Organoid Culture**—Crypt organoid culture and *Apc*-mutated organoid culture were performed based on the previous studies (Sato et al., 2011b; Sato et al., 2009). Briefly, the small intestine samples were opened longitudinally and washed with PBS several times. For extracting the crypt, the small intestine was incubated with 5mM EDTA/PBS for 30 min and the crypt-rich supernatant was collected after vigorous shaking. After filtering through the 100 strainers, the same number (300~500) of crypts were seeded in 50  $\mu$ l Matrigel (BD). 500  $\mu$ l of ENR medium (Advanced DMEM/F12 media supplement with EGF (20 ng/ml, Peprotech), Noggin (100 ng/ml, Peprotech) and R-spondin1 (500 ng/ml, Peprotech) were added every two days. For single cell organoid culture, crypts fractions collected through the 70  $\mu$ m (BD) cell strainer was incubated with Accumax (Stem cell technology 07921) and DNase (0.8 mg/ml, Sigma) for 30 min. Passaging through the 40  $\mu$ m strainer, ~5000 *Lgr5<sup>high</sup>* and Cytos Blue (Life technologies) negative cells were collected by cell sorting (MoFlo, Beckman Coulter) and seeded in Matrigel. ENR medium with Jagged-1 peptide (1  $\mu$ M, AnaSpec) was supplied every 2 days. Organoid efficiency was calculated by counting viable crypts or *Lgr5<sup>+</sup>* cells (at day 3) in total crypts (300~500 per well, crypt organoid) or total seeded cells (N=~2000 per well, single cell organoid). For *Apc<sup>Min/+</sup>* organoids, adenomas were collected and suspended with Advanced DMEM/F12 media supplement with EGF (20 ng/ml) and Noggin (100 ng/ml). Fresh media were supplemented every 3 days until the next passage (10-14 days). Cystic organoid efficiency was calculated by counting viable cells (at day 3) in total suspended cells (Single cell organoid). The size of organoids was analyzed by measuring the area of the middle section of organoids under the microscope using AxioVision software (Zeiss) (at least 30 organoids per group for all experiments).

**Organoid Retrovirus Infection**—For organoid gene transduction, we utilized the modified method based on the previous reference (Onuma et al., 2013). FACS sorted *Lgr5<sup>high</sup>* single cells (~5000) from *PAFWT* and *PAFKO* mice were incubated with media containing retroviruses expressing c-Myc with RFP (MSCV-c-Myc-IRES-RFP, Addgene [#35395]), or wild-type PAF and mutPIP-PAF (Jung et al., 2013) for 6h at 37 °C with polybrene (7  $\mu$ g/ml) and Jagged-1 peptide (1  $\mu$ M, AnaSpec). Then, infected cells were seeded on 50  $\mu$ L Matrigel/well in a 12-well plate with conventional ENR media. RFP+ cells were able to observe 2 days after infection. Only RFP+ cells were considered as transfected cells. For selecting nt-PAF or mutPIP-PAF infected organoids, blasticidin (10  $\mu$ g/ml) was treated.

**Lgr5 mRNA Fluorescence In Situ Hybridization (FISH)**—WT or *PAFKO* intestinal tissue sections (0 and 7 dpi) were processed for *Lgr5* mRNA FISH according to the manufacturer's protocol (Invitrogen, FISH Tag<sup>TM</sup> RNA Green Kit, with Alexa Fluor® 488 dye). Probe was designed as 530 base pair length targeting the coding sequence of *Lgr5*. A probe for sense strand was used as a negative control.

**Mammalian Cell Culture and Sphere Formation Assay**—CRC Cell line (HT29) was maintained in DMEM media containing 10% fetal bovine serum. For gene depletion, lentiviruses encoding short hairpins against *PAF mRNA* (MISSION shRNA, Sigma) were stably transduced into target cells and selected using puromycin (2 µg/ml). For counting the CSC population, trypsinized each cell line was counted and incubated with antibodies: CD44v6-APC (1:100, BD-Pharmingen [G44-26]) and CD133-FITC (1: 200, Miltenyi Biotec). Dead cells were excluded by Cyttox Blue staining. FACS analysis was performed using FacsJazz Cell Sorter (BD). For sphere formation assay, the limited number of HT-29 cells (5000 cells per ml) were plated in triplicate in the ultra-low attachment plates and grown for six days in serum-free stem cell medium (SCM) supplemented with B27 (Invitrogen), EGF (20 ng/ml, Invitrogen), and bFGF (10 ng/ml, Invitrogen). The number and size of spheres were quantified using AxioVision software (Zeiss).

**Chromatin Immunoprecipitation Assay**—The mouse small intestines (the duodenum) were minced and cross-linked with 1% formaldehyde for 15 min at room temperature. After quenching by glycine, samples were incubated with lysis buffer (0.5% NP40, HEPES 25 mM, KCl 150 mM, MgCl<sub>2</sub> 1.5 mM, 10% glycerol and KOH pH 7.5) containing proteinase inhibitors. Then the nuclear fractions were collected after centrifugation. Cell lysates were subjected to sonication (10 times, 30s on and 30s off, Bioruptor 300 [Diagenode]) with ChIP-lysis buffer (Tris 50 mM pH 8.0, NaCl 150 mM, 0.1% SDS, 0.5% deoxycholate, 1% NP40 and EDTA 1 mM). Supernatant from lysates was used for immunoprecipitation with the primary antibodies. The following antibodies were used for ChIP: RNA Polymerase II (1µg/ml, EMD Millipore [CTD4H8]), mouse-anti PAF (1 µg/ml, Abcam [ab56773]), and normal mouse IgG (1 µg/ml, Invitrogen). ChIP amplicons were detected by ChIP-PCR using the primers listed in STAR Methods.

**RNA-sequencing**—The total RNA from *Apc<sup>Min/+</sup>* and *PAF KO;Apc<sup>Min/+</sup>* adenomas (two biological replicas) were used for RNA-seq. The transcriptome sequencing was performed by BGI ([www.bgi.com/global/](http://www.bgi.com/global/)) with BGISEQ-500. Reads are mapped by Tophat2 and Differential genes are defined by Cuffdiff with P<0.05. KEGG analysis was performed by DAVID functional annotation analysis. GSEA analysis is performed with normalized FPKM of all genes with default parameters (Number of permutations =1000, collapse dataset=true, permutation type=phenotype).

## QUANTIFICATION AND STATISTICAL DETAILS

The Student *t*-test was applied for comparison of two samples. P-values below the 0.05 were considered significantly different. At least three biological and experimental replicas were used for statistical analyses, otherwise described in Figure legends. Error bars represent standard error (S.E.M).

## DATA AND SOFTWARE AVAILABILITY

The accession number for RNA-seq data reported in this paper is GSE109209. All data is available upon request.

## Supplementary Material

Refer to Web version on PubMed Central for supplementary material.

## Acknowledgments

We are grateful to Christopher Cervantes, Youn-Sang Jung, Seung-Hyo Lee, and Junjie Chen for helpful comments on the manuscript. This work was supported by the Cancer Prevention and Research Institute of Texas (RP140563), the National Institutes of Health (R01 CA193297-01), the Department of Defense (CA140572), the National Cancer Institute (P50 CA098258), the Duncan Family Institute Research Program, the University Cancer Foundation (IRG-08-061-01), the Center for Stem Cell and Developmental Biology (MD Anderson Cancer Center), an Institutional Research Grant (MD Anderson Cancer Center), a New Faculty Award (MD Anderson Cancer Center Support Grant), a Metastasis Research Center Grant (MD Anderson Cancer Center), and Uterine SPORE Career Enhancement Program (MD Anderson Cancer Center). The Genetically Engineered Mouse Facility was supported by the MD Anderson Cancer Center Support Grant (CA016672).

## References

- Araki R, Hoki Y, Uda M, Nakamura M, Jincho Y, Tamura C, Sunayama M, Ando S, Sugiura M, Yoshida MA, et al. Crucial role of c-Myc in the generation of induced pluripotent stem cells. *Stem Cells*. 2011; 29:1362–1370. [PubMed: 21732496]
- Asfaha S, Hayakawa Y, Muley A, Stokes S, Graham TA, Ericksen RE, Westphalen CB, von Burstin J, Mastracci TL, Worthley DL, et al. Krt19(+)/Lgr5(-) Cells Are Radioresistant Cancer-Initiating Stem Cells in the Colon and Intestine. *Cell Stem Cell*. 2015; 16:627–638. [PubMed: 26046762]
- Ashton GH, Morton JP, Myant K, Pheese TJ, Ridgway RA, Marsh V, Wilkins JA, Athineos D, Muncan V, Kemp R, et al. Focal adhesion kinase is required for intestinal regeneration and tumorigenesis downstream of Wnt/c-Myc signaling. *Dev Cell*. 2010; 19:259–269. [PubMed: 20708588]
- Barker N, Van Es JH, Kuipers J, Kujala P, Van Den Born M, Cozijnsen M, Haegerbarth A, Korving J, Begthel H, Peters PJ, et al. Identification of stem cells in small intestine and colon by marker gene Lgr5. *Nature*. 2007; 449:1003–1007. [PubMed: 17934449]
- Bettes MD, Dubois N, Murphy MJ, Dubey C, Roger C, Robine S, Trumpp A. c-Myc is required for the formation of intestinal crypts but dispensable for homeostasis of the adult intestinal epithelium. *Mol Cell Biol*. 2005; 25:7868–7878. [PubMed: 16107730]
- Buczacki SJA, Zecchini HI, Nicholson AM, Russell R, Vermeulen L, Kemp R, Winton DJ. Intestinal label-retaining cells are secretory precursors expressing lgr5. *Nature*. 2013; 495:65–69. [PubMed: 23446353]
- Cadigan KM, Waterman ML. TCF/LEFs and Wnt signaling in the nucleus. *Cold Spring Harb Perspect Biol*. 2012; 4
- Cheng Y, Li K, Diao D, Zhu K, Shi L, Zhang H, Yuan D, Guo Q, Wu X, Liu D, et al. Expression of KIAA0101 protein is associated with poor survival of esophageal cancer patients and resistance to cisplatin treatment in vitro. *Laboratory Investigation*. 2013; 93:1276–1287. [PubMed: 24145239]
- Clevers H, Nusse R. Wnt/beta-catenin signaling and disease. *Cell*. 2012; 149:1192–1205. [PubMed: 22682243]
- De Biasio A, de Opakua AI, Mortuza GB, Molina R, Cordeiro TN, Castillo F, Villate M, Merino N, Delgado S, Gil-Carton D, et al. Structure of p15(PAF)-PCNA complex and implications for clamp sliding during DNA replication and repair. *Nat Commun*. 2015; 6:6439. [PubMed: 25762514]
- Dean M, Fojo T, Bates S. Tumour stem cells and drug resistance. *Nat Rev Cancer*. 2005; 5:275–284. [PubMed: 15803154]
- Emanuele MJ, Ciccio A, Elia AEH, Elledge SJ. Proliferating cell nuclear antigen (PCNA)-associated KIAA0101/PAF15 protein is a cell cycle-regulated anaphase-promoting complex/cyclosome substrate. *Proceedings of the National Academy of Sciences of the United States of America*. 2011; 108:9845–9850. [PubMed: 21628590]
- Erismann MD, Rothberg PG, Diehl RE, Morse CC, Spandorfer JM, Astrin SM. Deregulation of c-myc gene expression in human colon carcinoma is not accompanied by amplification or rearrangement of the gene. *Mol Cell Biol*. 1985; 5:1969–1976. [PubMed: 3837853]



- Fuchs E, Tumber T, Guasch G. Socializing with the neighbors: stem cells and their niche. *Cell*. 2004; 116:769–778. [PubMed: 15035980]
- Hosen N, Yamane T, Muijtjens M, Pham K, Clarke MF, Weissman IL. Bmi-1-green fluorescent protein-knock-in mice reveal the dynamic regulation of bmi-1 expression in normal and leukemic hematopoietic cells. *Stem Cells*. 2007; 25:1635–1644. [PubMed: 17395774]
- Hosokawa M, Takehara A, Matsuda K, Eguchi H, Ohigashi H, Ishikawa O, Shinomura Y, Imai K, Nakamura Y, Nakagawa H. Oncogenic role of KIAA0101 interacting with proliferating cell nuclear antigen in pancreatic cancer. *Cancer Research*. 2007; 67:2568–2576. [PubMed: 17363575]
- Jain M, Zhang L, Patterson EE, Kebebew E. KIAA0101 is overexpressed, and promotes growth and invasion in adrenal cancer. *PLoS ONE*. 2011; 6
- Jun S, Jung YS, Suh HN, Wang W, Kim MJ, Oh YS, Lien EM, Shen X, Matsumoto Y, McCrea PD, et al. LIG4 mediates Wnt signalling-induced radioresistance. *Nat Commun*. 2016; 7:10994. [PubMed: 27009971]
- Jun S, Lee S, Kim HC, Ng C, Schneider AM, Ji H, Ying H, Wang H, DePinho RA, Park JI. PAF-mediated MAPK signaling hyperactivation via LAMTOR3 induces pancreatic tumorigenesis. *Cell Rep*. 2013; 5:314–322. [PubMed: 24209743]
- Jung HY, Jun S, Lee M, Kim HC, Wang X, Ji H, McCrea PD, Park JI. PAF and EZH2 induce wnt/ $\beta$ -catenin signaling hyperactivation. *Molecular Cell*. 2013; 52:193–205. [PubMed: 24055345]
- Kais Z, Barsky SH, Mathsyaraja H, Zha A, Ransburgh DJR, He G, Pilarski RT, Shapiro CL, Huang K, Parvin JD. KIAA0101 interacts with BRCA1 and regulates centrosome number. *Molecular Cancer Research*. 2011; 9:1091–1099. [PubMed: 21673012]
- Kato T, Daigo Y, Aragaki M, Ishikawa K, Sato M, Kaji M. Overexpression of KIAA0101 predicts poor prognosis in primary lung cancer patients. *Lung Cancer*. 2012; 75:110–118. [PubMed: 21689861]
- Kemper K, Sprick MR, de Bree M, Scopelliti A, Vermeulen L, Hoek M, Zeilstra J, Pals ST, Mehmet H, Stassi G, et al. The AC133 epitope, but not the CD133 protein, is lost upon cancer stem cell differentiation. *Cancer Res*. 2010; 70:719–729. [PubMed: 20068153]
- Kreso A, Dick JE. Evolution of the cancer stem cell model. *Cell Stem Cell*. 2014; 14:275–291. [PubMed: 24607403]
- Laurenti E, Varnum-Finney B, Wilson A, Ferrero I, Blanco-Bose WE, Ehninger A, Knoepfler PS, Cheng PF, MacDonald HR, Eisenman RN, et al. Hematopoietic Stem Cell Function and Survival Depend on c-Myc and N-Myc Activity. *Cell Stem Cell*. 2008; 3:611–624. [PubMed: 19041778]
- Metcalf C, Kljavin NM, Ybarra R, De Sauvage FJ. Lgr5+ stem cells are indispensable for radiation-induced intestinal regeneration. *Cell Stem Cell*. 2014; 14:149–159. [PubMed: 24332836]
- Mizutani K, Onda M, Asaka S, Akaishi J, Miyamoto S, Yoshida A, Nagahama M, Ito K, Emi M. Overexpressed in anaplastic thyroid carcinoma-1 (OEATC-1) as a novel gene responsible for anaplastic thyroid carcinoma. *Cancer*. 2005; 103:1785–1790. [PubMed: 15789362]
- Montgomery RK, Carlone DL, Richmond CA, Farilla L, Kranendonk MEG, Henderson DE, Baffour-Awuah NY, Ambruzs DM, Fogli LK, Algra S, et al. Mouse telomerase reverse transcriptase (mTert) expression marks slowly cycling intestinal stem cells. *Proceedings of the National Academy of Sciences of the United States of America*. 2011; 108:179–184. [PubMed: 21173232]
- Morrison SJ, Spradling AC. Stem cells and niches: mechanisms that promote stem cell maintenance throughout life. *Cell*. 2008; 132:598–611. [PubMed: 18295578]
- Moser AR, Pitot HC, Dove WF. A dominant mutation that predisposes to multiple intestinal neoplasia in the mouse. *Science*. 1990; 247:322–324. [PubMed: 2296722]
- Muñoz J, Stange DE, Schepers AG, Van De Wetering M, Koo BK, Itzkovitz S, Volckmann R, Kung KS, Koster J, Radulescu S, et al. The Lgr5 intestinal stem cell signature: Robust expression of proposed quiescent ‘+4’ cell markers. *EMBO Journal*. 2012; 31:3079–3091. [PubMed: 22692129]
- Munoz NM, Upton M, Rojas A, Washington MK, Lin L, Chytil A, Sozmen EG, Madison BB, Pozzi A, Moon RT, et al. Transforming growth factor beta receptor type II inactivation induces the malignant transformation of intestinal neoplasms initiated by Apc mutation. *Cancer Res*. 2006; 66:9837–9844. [PubMed: 17047044]
- Nguyen LV, Vanner R, Dirks P, Eaves CJ. Cancer stem cells: an evolving concept. *Nat Rev Cancer*. 2012; 12:133–143. [PubMed: 22237392]

- Nie Z, Hu G, Wei G, Cui K, Yamane A, Resch W, Wang R, Green DR, Tessarollo L, Casellas R, et al. c-Myc is a universal amplifier of expressed genes in lymphocytes and embryonic stem cells. *Cell*. 2012; 151:68–79. [PubMed: 23021216]
- O'Brien CA, Pollett A, Gallinger S, Dick JE. A human colon cancer cell capable of initiating tumour growth in immunodeficient mice. *Nature*. 2007; 445:106–110. [PubMed: 17122772]
- Onuma K, Ochiai M, Orihashi K, Takahashi M, Imai T, Nakagama H, Hippo Y. Genetic reconstitution of tumorigenesis in primary intestinal cells. *Proc Natl Acad Sci U S A*. 2013; 110:11127–11132. [PubMed: 23776211]
- Polakis P. Drugging Wnt signalling in cancer. *EMBO J*. 2012; 31:2737–2746. [PubMed: 22617421]
- Povlsen LK, Beli P, Wagner SA, Poulsen SL, Sylvestersen KB, Poulsen JW, Nielsen ML, Bekker-Jensen S, Mailand N, Choudhary C. Systems-wide analysis of ubiquitylation dynamics reveals a key role for PAF15 ubiquitylation in DNA-damage bypass. *Nature Cell Biology*. 2012; 14:1089–1098. [PubMed: 23000965]
- Powell AE, Wang Y, Li Y, Poulin EJ, Means AL, Washington MK, Higginbotham JN, Juchheim A, Prasad N, Levy SE, et al. The pan-ErbB negative regulator Irig1 is an intestinal stem cell marker that functions as a tumor suppressor. *Cell*. 2012; 149:146–158. [PubMed: 22464327]
- Ricci-Vitiani L, Lombardi DG, Pilozzi E, Biffoni M, Todaro M, Peschle C, De Maria R. Identification and expansion of human colon-cancer-initiating cells. *Nature*. 2007; 445:111–115. [PubMed: 17122771]
- Sangiorgi E, Capecchi MR. Bmi1 is expressed in vivo in intestinal stem cells. *Nature Genetics*. 2008; 40:915–920. [PubMed: 18536716]
- Sansom OJ, Meniel VS, Muncan V, Pheasant TJ, Wilkins JA, Reed KR, Vass JK, Athineos D, Clevers H, Clarke AR. Myc deletion rescues Apc deficiency in the small intestine. *Nature*. 2007; 446:676–679. [PubMed: 17377531]
- Sato T, Stange DE, Ferrante M, Vries RG, Van Es JH, Van den Brink S, Van Houdt WJ, Pronk A, Van Gorp J, Siersema PD, et al. Long-term expansion of epithelial organoids from human colon, adenoma, adenocarcinoma, and Barrett's epithelium. *Gastroenterology*. 2011a; 141:1762–1772. [PubMed: 21889923]
- Sato T, Van Es JH, Snippert HJ, Stange DE, Vries RG, Van Den Born M, Barker N, Shroyer NF, Van De Wetering M, Clevers H. Paneth cells constitute the niche for Lgr5 stem cells in intestinal crypts. *Nature*. 2011b; 469:415–418. [PubMed: 21113151]
- Sato T, Vries RG, Snippert HJ, van de Wetering M, Barker N, Stange DE, van Es JH, Abo A, Kujala P, Peters PJ, et al. Single Lgr5 stem cells build crypt-villus structures in vitro without a mesenchymal niche. *Nature*. 2009; 459:262–265. [PubMed: 19329995]
- Schepers AG, Snippert HJ, Stange DE, van den Born M, van Es JH, van de Wetering M, Clevers H. Lineage tracing reveals Lgr5+ stem cell activity in mouse intestinal adenomas. *Science*. 2012; 337:730–735. [PubMed: 22855427]
- Sikora K, Chan S, Evan G, Gabra H, Markham N, Stewart J, Watson J. c-myc oncogene expression in colorectal cancer. *Cancer*. 1987; 59:1289–1295. [PubMed: 3545431]
- Suh HN, Kim MJ, Jung YS, Lien EM, Jun S, Park JI. Quiescence Exit of Tert(+) Stem Cells by Wnt/beta-Catenin Is Indispensable for Intestinal Regeneration. *Cell Rep*. 2017; 21:2571–2584. [PubMed: 29186692]
- Takahashi K, Tanabe K, Ohnuki M, Narita M, Ichisaka T, Tomoda K, Yamanaka S. Induction of pluripotent stem cells from adult human fibroblasts by defined factors. *Cell*. 2007; 131:861–872. [PubMed: 18035408]
- Takaku K, Oshima M, Miyoshi H, Matsui M, Seldin MF, Taketo MM. Intestinal tumorigenesis in compound mutant mice of both Dpc4 (Smad4) and Apc genes. *Cell*. 1998; 92:645–656. [PubMed: 9506519]
- Takeda N, Jain R, LeBoeuf MR, Wang Q, Lu MM, Epstein JA. Interconversion between intestinal stem cell populations in distinct niches. *Science*. 2011; 334:1420–1424. [PubMed: 22075725]
- Tetteh PW, Basak O, Farin HF, Wiebrands K, Kretzschmar K, Begthel H, Van Den Born M, Korving J, De Sauvage F, Van Es JH, et al. Replacement of Lost Lgr5-Positive Stem Cells through Plasticity of Their Enterocyte-Lineage Daughters. *Cell Stem Cell*. 2016; 18:203–213. [PubMed: 26831517]

- Tian H, Biehs B, Warming S, Leong KG, Rangell L, Klein OD, De Sauvage FJ. A reserve stem cell population in small intestine renders Lgr5-positive cells dispensable. *Nature*. 2011; 478:255–259. [PubMed: 21927002]
- van Es JH, Jay P, Gregorieff A, van Gijn ME, Jonkheer S, Hatzis P, Thiele A, van den Born M, Begthel H, Brabletz T, et al. Wnt signalling induces maturation of Paneth cells in intestinal crypts. *Nature Cell Biology*. 2005; 7:381–386. [PubMed: 15778706]
- Van Es JH, Sato T, Van De Wetering M, Lyubimova A, Yee Nee AN, Gregorieff A, Sasaki N, Zeinstra L, Van Den Born M, Korving J, et al. Dll1 + secretory progenitor cells revert to stem cells upon crypt damage. *Nature Cell Biology*. 2012; 14:1099–1104. [PubMed: 23000963]
- Varlakhanova NV, Cotterman RF, deVries WN, Morgan J, Donahue LR, Murray S, Knowles BB, Knoepfler PS. *myc* maintains embryonic stem cell pluripotency and self-renewal. *Differentiation*. 2010; 80:9–19. [PubMed: 20537458]
- Varnat F, Duquet A, Malerba M, Zbinden M, Mas C, Gervaz P, Ruiz i Altaba A. Human colon cancer epithelial cells harbour active HEDGEHOG–GLI signalling that is essential for tumour growth, recurrence, metastasis and stem cell survival and expansion. *EMBO Mol Med*. 2009; 1:338–351. [PubMed: 20049737]
- Wang H, Yang H, Shivalila CS, Dawlaty MM, Cheng AW, Zhang F, Jaenisch R. One-step generation of mice carrying mutations in multiple genes by CRISPR/Cas-mediated genome engineering. *Cell*. 2013; 153:910–918. [PubMed: 23643243]
- Wang X, Jung YS, Jun S, Lee S, Wang W, Schneider A, Sun Oh Y, Lin SH, Park BJ, Chen J, et al. PAF-Wnt signaling-induced cell plasticity is required for maintenance of breast cancer cell stemness. *Nature Communications*. 2016; 7
- Wilson A, Murphy MJ, Oskarsson T, Kaloulis K, Bettess MD, Oser GM, Pasche AC, Knabenhans C, Macdonald HR, Trumpp A. c-Myc controls the balance between hematopoietic stem cell self-renewal and differentiation. *Genes Dev*. 2004; 18:2747–2763. [PubMed: 15545632]
- Yang H, Wang H, Shivalila CS, Cheng AW, Shi L, Jaenisch R. One-step generation of mice carrying reporter and conditional alleles by CRISPR/Cas-mediated genome engineering. *Cell*. 2013; 154:1370–1379. [PubMed: 23992847]
- Yu P, Huang B, Shen M, Lau C, Chan E, Michel J, Xiong Y, Payan DG, Luo Y. p15PAF, a novel PCNA associated factor with increased expression in tumor tissues. *Oncogene*. 2001; 20:484–489. [PubMed: 11313979]
- Yuan RH, Jeng YM, Pan HW, Hu FC, Lai PL, Lee PH, Hsu HC. Overexpression of KIAA0101 predicts high stage, early tumor recurrence, and poor prognosis of hepatocellular carcinoma. *Clinical Cancer Research*. 2007; 13:5368–5376. [PubMed: 17875765]
- Zeilstra J, Joosten SPJ, Dokter M, Verwiel E, Spaargaren M, Pals ST. Deletion of the WNT target and cancer stem cell marker CD44 in *Apc(Min/+)* mice attenuates intestinal tumorigenesis. *Cancer Research*. 2008; 68:3655–3661. [PubMed: 18483247]
- Zhu L, Gibson P, Currie DS, Tong Y, Richardson RJ, Bayazitov IT, Poppleton H, Zakharenko S, Ellison DW, Gilbertson RJ. Prominin 1 marks intestinal stem cells that are susceptible to neoplastic transformation. *Nature*. 2009; 457:603–607. [PubMed: 19092805]

**HIGHLIGHTS**

- PAF is expressed in intestinal stem cells and upregulated in regenerating crypts
- PAF transactivates *c-Myc* in intestinal stem cells of the regenerating crypts
- PAF-Myc axis is required for intestinal regeneration
- PAF-Myc axis is required for stemness of colorectal cancer cells

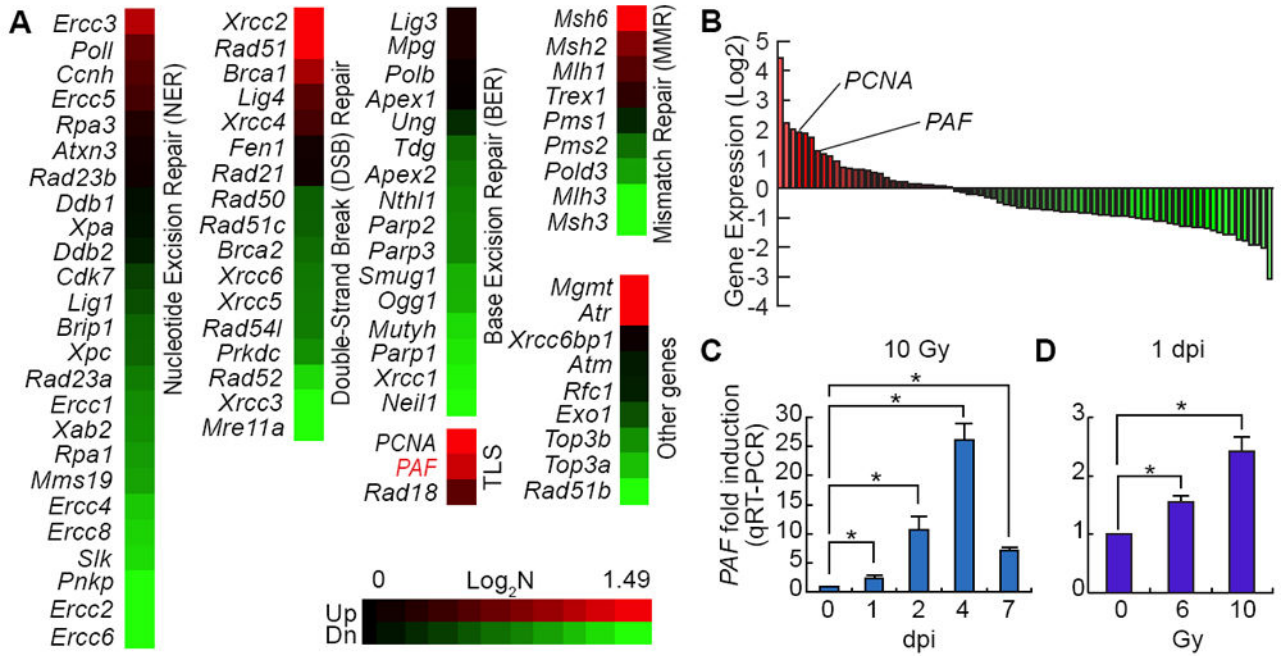


**Figure 1. Upregulation of PAF Expression upon Radiation Injury**

(A, B) Gene expression profiling of DNA repair genes upon radiation injury in mouse small intestine. After treatment of 10 Gy irradiation (1 day post-injury [1 dpi]), the whole small intestine samples were analyzed by qRT-PCR (N=3). *PCNA* is the fourth and *PAF* are the seventh upregulated genes among the 79 genes related to DNA repair.

(C) Time-dependent upregulation of *PAF* expression upon IR injury. At 0, 1, 2, 4, and 7 dpi, the small intestine samples were collected and analyzed by qRT-PCR (N=3).

(D) Dose-dependent upregulation of *PAF* expression upon injury. 6 and 10 Gy irradiation were used (1 dpi). Student's *t*-test; error bars = S.E.M; asterisks:  $P < 0.05$ .



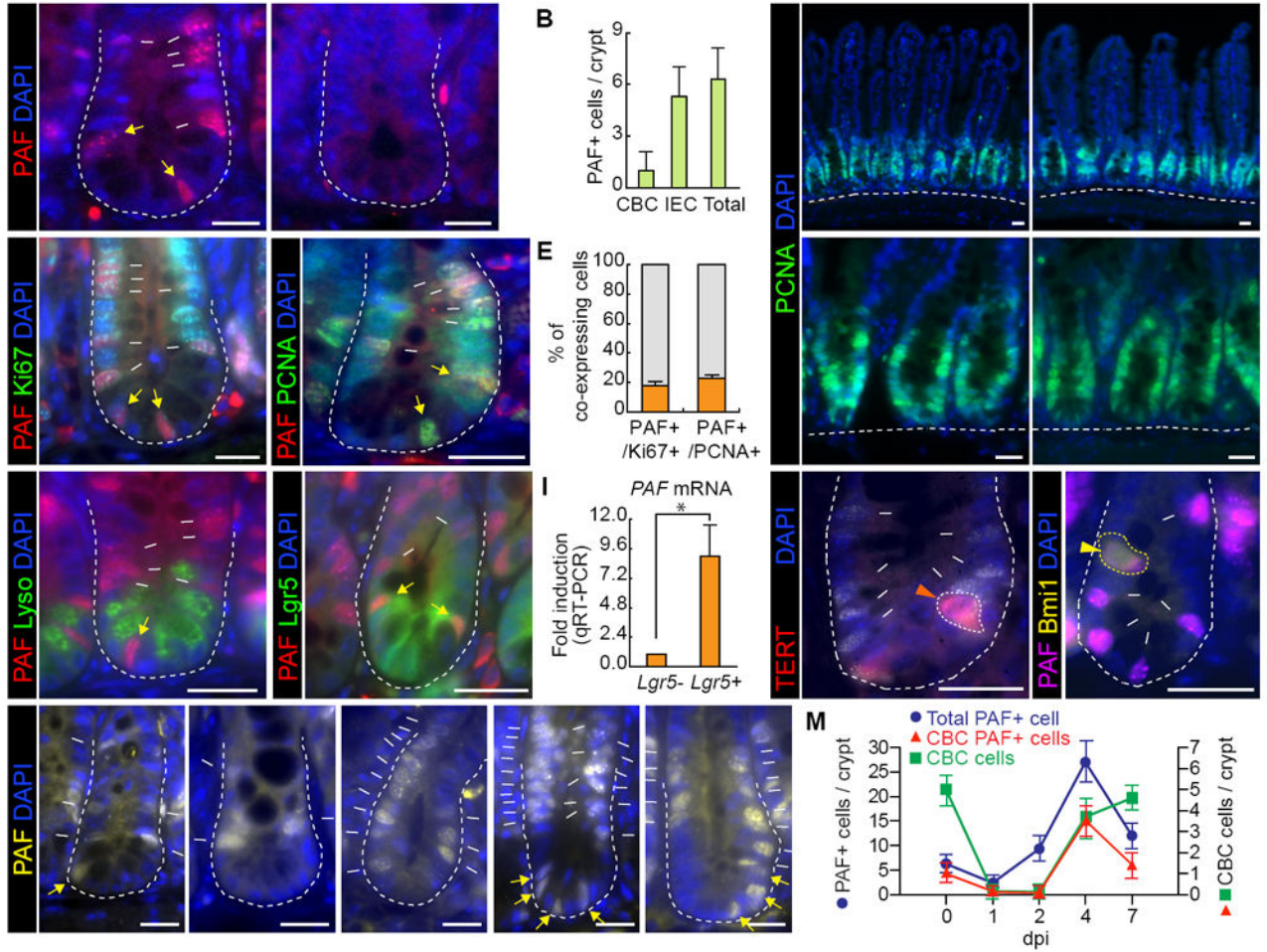


**Figure 2. PAF Expression in Normal and Regenerating Intestinal Crypts**

(A) PAF expression in the small intestine. *PAF*WT and KO mice were analyzed for immunofluorescent (IF) staining of PAF (arrows). Asterisks mark non-specific staining signals.

(B) Quantification of PAF+ cells in the small intestinal crypts.

(C) Co-immunostaining of mouse small intestine (*PAF*WT and KO) for PAF and Ki67. White arrows: PAF+:Ki67+ cells; yellow arrows: PAF+:Ki67+ CBC cells. Asterisks mark non-specific staining signals.

(D) Co-immunostaining of mouse small intestine (*PAF*WT and KO) for PAF and PCNA. White arrows: PAF+:PCNA+ cells; yellow arrows: PAF+:PCNA+ CBC cells; Asterisks mark non-specific staining signals.

(E) Quantification of PAF+ cells in K67+ or PCNA+ cell population. Of note, PAF+:Ki67- cells were rarely found (approximately 1/50 crypts).

(F) No effects of *PAF*KO on PCNA expression pattern. IF staining of the mouse small intestine for PCNA.

(G) No expression of PAF in the Paneth cells. Co-immunostaining of the small intestine for PAF and Lysozyme. White arrows: PAF+ cells; yellow arrows: PAF+ CBC cell.



(H) Co-expression of PAF and *Lgr5* in the small intestine. Co-immunostaining of the small intestine of *Lgr5-EGFP-CreERT2* mouse strain. White arrows: PAF+:*Lgr5*+ cells; yellow arrows: PAF+:*Lgr5*+ CBC cells. Asterisks indicate non-specific staining signals.

(I) *PAF* expression in *Lgr5*+ cells. FACS-isolated *Lgr5*+ cells were analyzed for qRT-PCR. Asterisk= $P<0.05$ .

(J, K) PAF expression in *TERT*+ and *Bmi1*+ cells. Co-immunostaining of *TERT-Tdtomato-CreERT2* or *Bmi1-EGFP* knock-in mouse intestine samples for PAF. Arrowheads: PAF+:*TERT*+ (J) and PAF+:*Bmi1*+ (K) cells; arrows: PAF+ cells. Asterisks mark non-specific staining signals.

(L, M) The increase of PAF+ cells upon radiation injury. Immunostaining of mouse intestine (0, 1, 2, 4, and 7 dpi; 10 Gy) for PAF (L). White arrows: PAF+ cells; yellow arrows: PAF+ CBC cells. Quantification of PAF+ cells in the regenerating crypts (M).

The representative images were shown from at least three independent experiments. Scale bars=20 $\mu$ m. See also Figures S1 and S2.

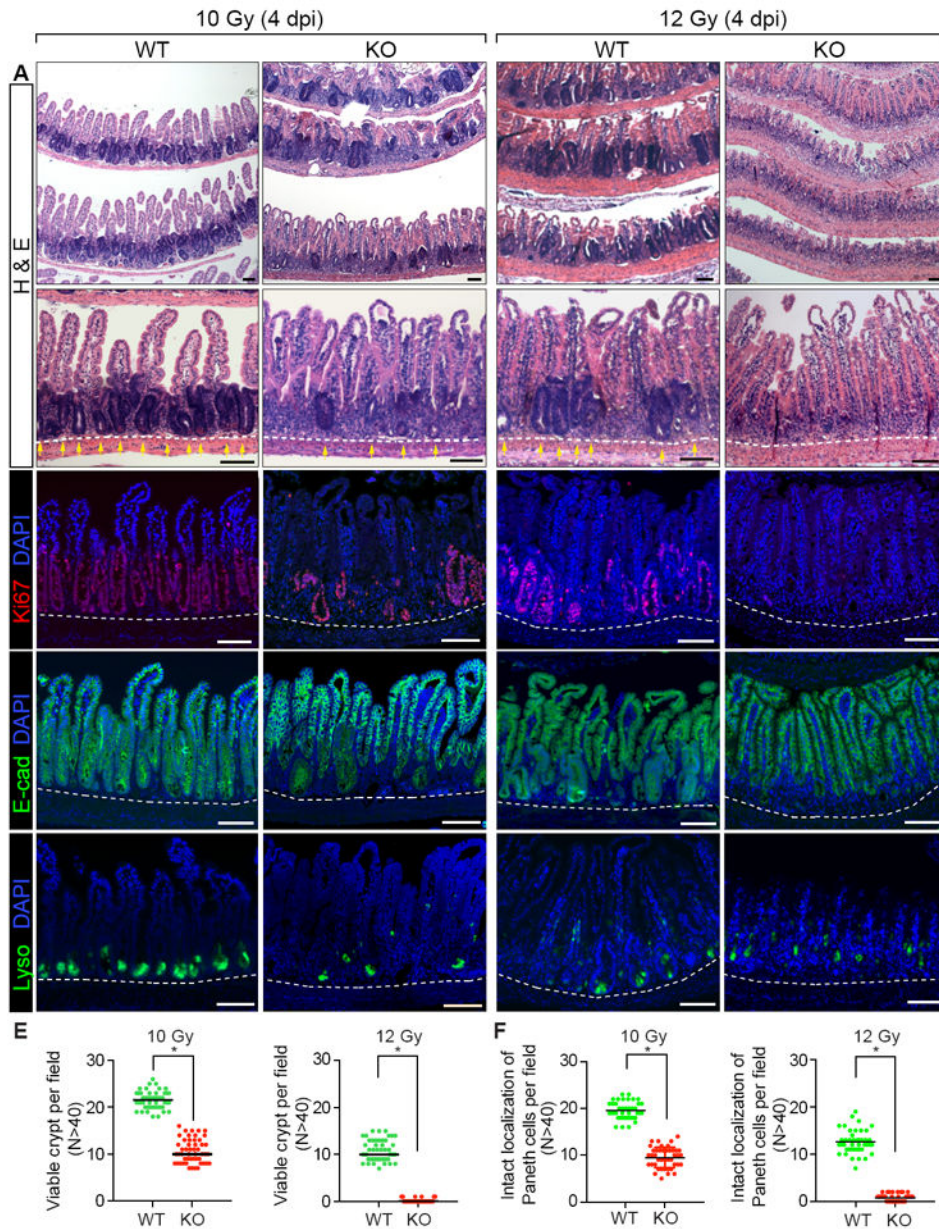


### Figure 3. Impaired Intestinal Regeneration by *PAF* KO

(A-D) Impaired intestinal regeneration after irradiation (4 dpi; 10 and 12 Gy). Hematoxylin and eosin staining of the mouse small intestine samples of *PAF*<sup>+/+</sup> (WT) or *PAF*<sup>-/-</sup> (KO) mice (A); IHC of the small intestine samples for Ki67 (B); IHC of the small intestine samples for E-cadherin, a marker for epithelial cell (C); IHC of the small intestine samples for Lysozyme, a marker for Paneth cell (D); Yellow arrows: crypts.

(E) Quantification of the viable crypts. Crypts that showed five successive Ki67+ cells were counted as a viable crypt.

(D) Quantification of the intact localization of Lysozyme. Crypts possessing at least three Lyso+ cells localized at the crypt bottom were counted as intact localization.

The representative images were shown from at least three animals for each condition. Scale bars=100 $\mu$ m. See also Figures S3 and S4.

Author Manuscript

Author Manuscript

Author Manuscript

Author Manuscript

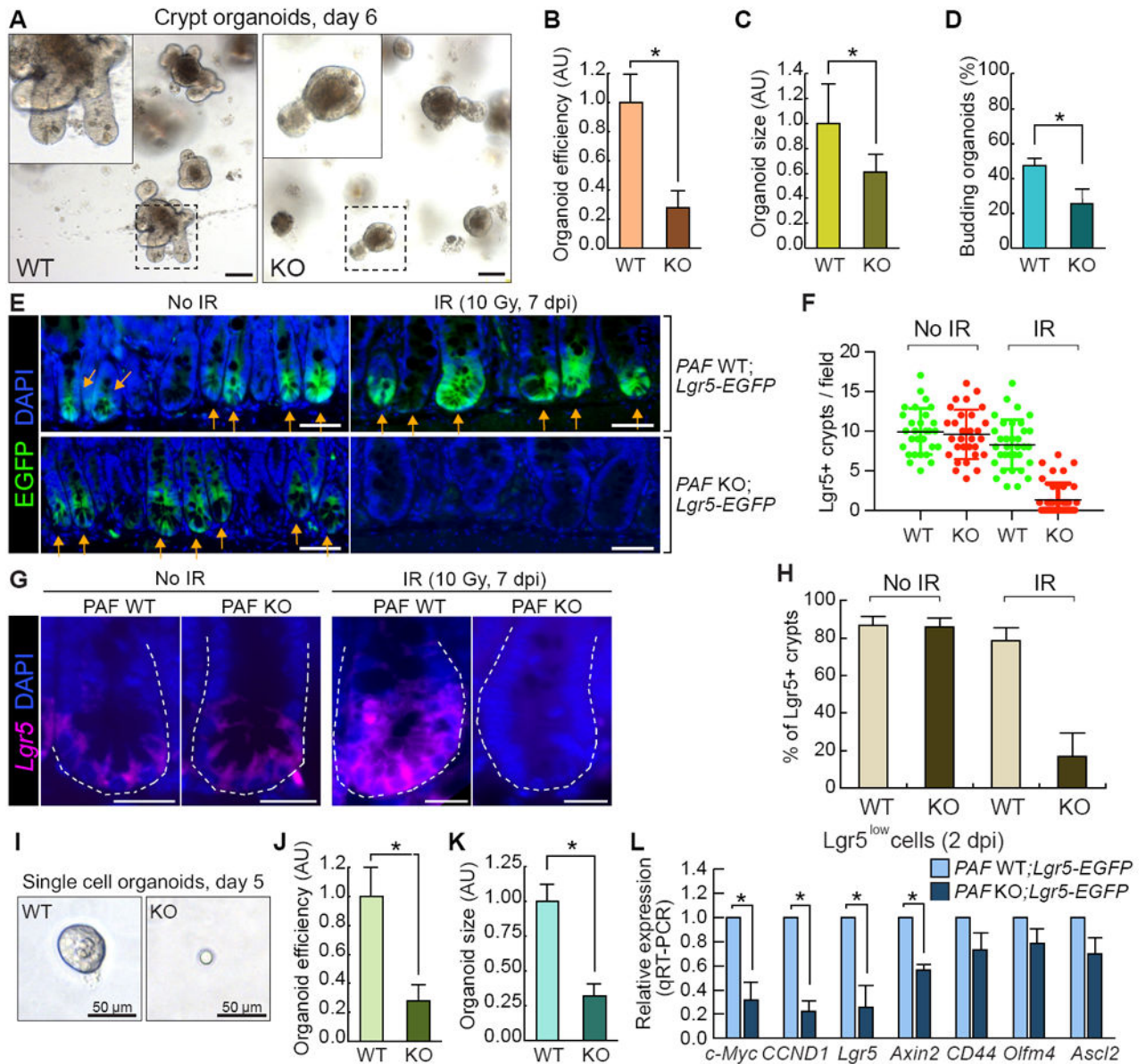


#### Figure 4. PAF Is Required for ISC/IPC Expansion in Regenerating Crypts

(A-D) Reduced organoid development by *PAFKO*. The crypt organoid growth assays from the small intestine samples of *PAFWT* and *PAFKO* mice (A); quantification of organoid efficiency (N = 2000 from the three independent experiments) (B); size (5 days after seeding; N = 50) (C); budding efficiency (N = 50) (D). Asterisks= $P < 0.01$ . Scale bars=100 $\mu$ m.

(E, F) Impaired ISC/IPC expansion by *PAFKO*. Visualization of Lgr5+ EGFP cells by GFP immunostaining of the small intestines from *PAFWT*; *Lgr5-EGFP* and *PAFKO*; *Lgr5-EGFP* mice at 0 and 7 dpi (E). Scale bars=50 $\mu$ m; Quantification Lgr5+ (EGFP+) existing crypts per field (F). At least 30 fields of view were counted; Arrows (EGFP+ crypts); asterisks (EGFP-regenerating crypts).

(G, H) Analysis of *Lgr5* expression by FISH in *PAFWT* and *PAFKO* regeneration crypts. The representative images were shown. (G). Scale bars=20 $\mu$ m; % of *Lgr5*<sup>+</sup> (EGFP<sup>+</sup>) crypts in the field (H). At least 10 fields of view were counted.

(I-K) Reduced single cell organoid development by *PAFKO*. Representative images of single cell (*Lgr5*<sup>+</sup>) organoids (day 5) derived from *PAFWT;Lgr5-EGFP* and *PAFKO;Lgr5-EGFP* mice (I). Scale bars=50 $\mu$ m; quantification of organoid development efficiency (J) (N 5000 cells were analyzed for from three independent experiments); size (K) (N 30 single cell organoids were analyzed). (L) Gene expression analysis of FACS-isolated *Lgr5*<sup>low</sup> (GFP<sup>+</sup>) cells in the IR-treated intestine from *PAFWT;Lgr5-EGFP* and *PAFKO;Lgr5-EGFP* mice (2 dpi, 10 Gy). qRT-PCR analysis. Asterisks=P< 0.05. See also Figure S5.



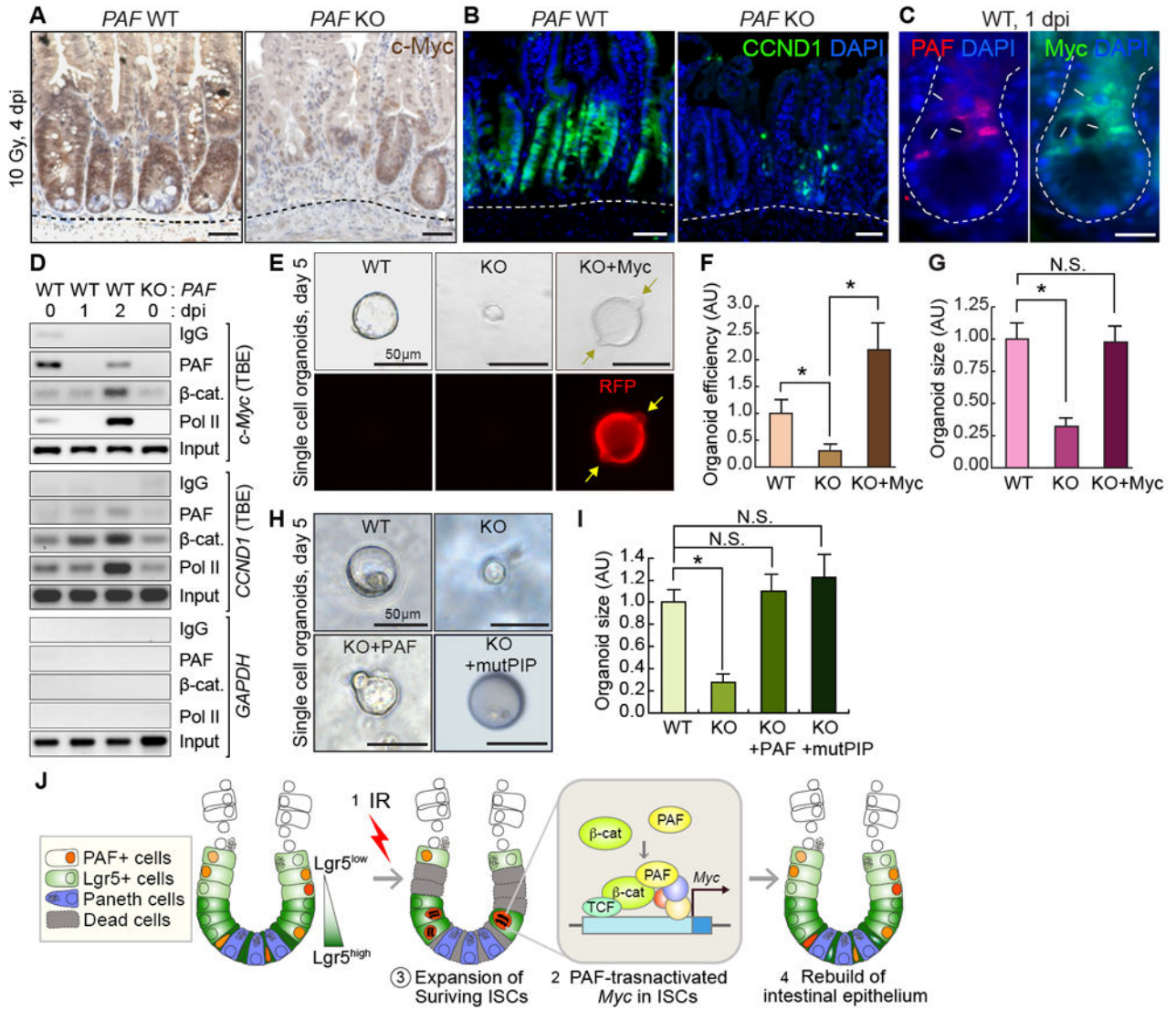


**Figure 5. Requirement of PAF-Myc Axis for ISCs/IPCs Expansion**

(A, B) Downregulation of c-Myc and Cyclin D1 in *PAFKO* crypts (4 dpi, 10 Gy). IHC for c-Myc or Cyclin D1. Hematoxylin or DAPI for nuclear counterstaining (blue).

(C) Co-expression of PAF and c-Myc in surviving cells in the regenerating crypts. Arrows: PAF+:Myc+ cells; asterisks: disappeared CBC cells.

(D) Conditional recruitment of PAF and  $\beta$ -catenin to TCF-binding elements (TBEs) in *c-Myc* and *CCND1* (*Cyclin D1*) proximal promoter. Chromatin immunoprecipitation (ChIP) assays of the mouse small intestine (*PAF* WT and KO; 1 and 2 dpi; 10 Gy). IgG ChIP and *PAFKO* small intestine samples served as negative control. RNA Pol II ChIP (positive control for gene transactivation). *GAPDH* promoter served as negative control.

(E-G) Rescue of *PAFKO*-induced organoid growth failure by c-Myc expression. The Lgr5+ cells isolated from (*PAF* WT and KO) were transduced with Retroviruses encoding c-Myc and RFP (red fluorescent protein) and cultured for organoid development. Arrows indicate



the budding. The representative images (E); quantification of organoid efficiency (F) and size (G). Asterisks:  $P < 0.05$  (N = 30). N.S. (not significant;  $P > 0.05$ ).

(H, I) Rescue of *PAF*KO-induced organoid growth failure by ectopic expression of wild-type PAF and PIP mutant PAF (mutPIP-PAF). The *Lgr5*<sup>+</sup> cells isolated from *PAF*KO;*Lgr5*-*EGFP* were transduced with retroviruses encoding wild-type PAF and mutPIP-PAF and cultured for organoid development. The representative images (H); Quantification of organoid size (I) Asterisks:  $P < 0.05$  (N = 20).

(J) Illustration of the working model. Upon irradiation injury, the highly proliferative cells (*Lgr5*<sup>high</sup> ISCs and some of *Lgr5*<sup>low</sup> TA cells) undergo apoptosis. PAF and  $\beta$ -catenin transactivate *c-Myc* in the surviving ISCs/IPC (s) (*Lgr5*<sup>low</sup>), which leads to the expansion of ISCs/IPC (s) and the subsequent rebuilding of the intestinal epithelium. Scale bars=50 $\mu$ m (A, B, E, H) and 20 $\mu$ m (C); the representative images were shown from at least three independent experiments. See also Figure S5

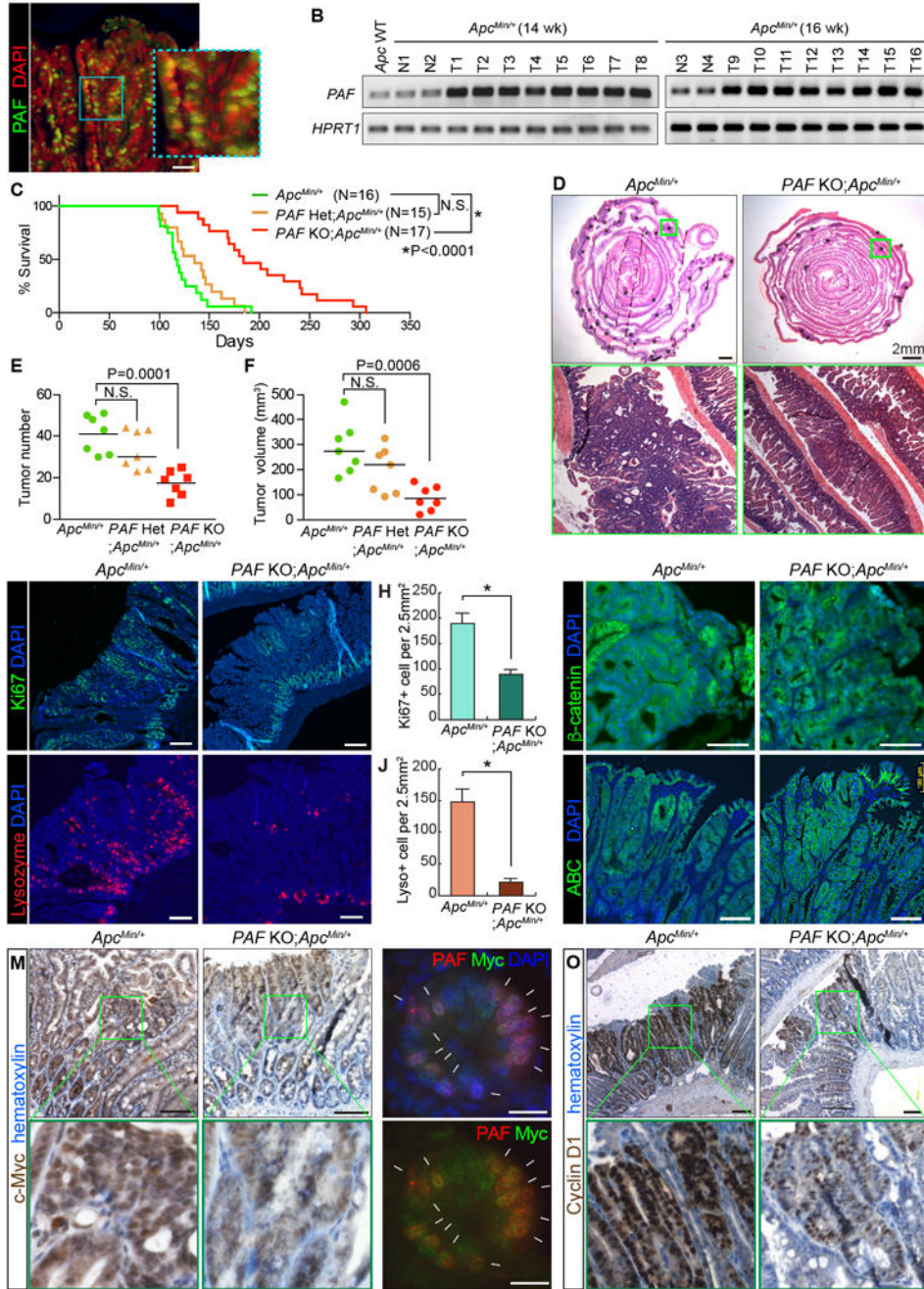


**Figure 6. Attenuation of Intestinal Tumorigenesis by PAF KO**

(A, B) Expression of PAF in *Apc<sup>Min/+</sup>* adenomas. Immunostaining of *Apc<sup>Min/+</sup>* intestinal adenoma (16 wk old) (A), scale bar=50µm; semi-RT-PCR (B). *Apc* WT: Wild-type (*Apc<sup>+/+</sup>*) intestine sample; N1-4: normal adjacent intestine samples; T1-16: intestinal adenomas. (C) The extended life span of *Apc<sup>Min/+</sup>* mice by PAF KO. Kaplan-Meier survival curve of *Apc<sup>Min/+</sup>* (N=16), *PAF Het;Apc<sup>Min/+</sup>* (N=15), and *PAF KO;Apc<sup>Min/+</sup>* (N=17). (D) H&E staining of the small intestines from *Apc<sup>Min/+</sup>* and *PAF KO;Apc<sup>Min/+</sup>* (age of 16 weeks). Asterisks indicate intestinal adenomas. Scale bars=2mm.

(E, F) Decreased tumor burden of *Apc<sup>Min/+</sup>* mice by *PAFKO*. The number of tumors (< 1.5mm) (E) and tumor volumes (mm<sup>3</sup>) (F) were quantified; 16 wk old; N=7 for each group.

(G, H) Reduced cell proliferation of *Apc<sup>Min</sup>* tumors by *PAFKO*. Ki67 staining of small intestine adenomas from *Apc<sup>Min/+</sup>* or *PAFKO;Apc<sup>Min/+</sup>* (16 wk old) (G); quantification (H). Asterisk: P<0.001.

(I, J) Decreased differentiation of the Paneth cells of *Apc<sup>Min</sup>* tumors by *PAFKO*. Lysozyme staining of small intestine adenomas from *Apc<sup>Min/+</sup>* or *PAFKO;Apc<sup>Min/+</sup>* (16 wk old) (I); quantification (J). Asterisk: P<0.001.

(K, L) No change in  $\beta$ -catenin level and activity of *Apc<sup>Min</sup>* tumors by *PAFKO*. Immunostaining of small intestine adenomas from *Apc<sup>Min/+</sup>* or *PAFKO;Apc<sup>Min/+</sup>* (16wk old) for total  $\beta$ -catenin (K) and active (unphosphorylated)  $\beta$ -catenin (ABC) (L). Scale bars=100 $\mu$ m.

(M) Downregulation of c-Myc of *Apc<sup>Min</sup>* tumors by *PAFKO*. c-Myc IHC; 16 wk old. Scale bars=100 $\mu$ m.

(N) Co-expression of c-Myc and PAF in *Apc<sup>Min</sup>* tumors. Arrows: PAF+:Myc+ cells. Scale bars=20 $\mu$ m.

(O) Downregulation of Cyclin D1 of *Apc<sup>Min</sup>* tumors by *PAFKO*. Cyclin D1 IHC; 16 wk old. Scale bars=100 $\mu$ m.

The representative images (N 3) were shown. See also Figure S6.

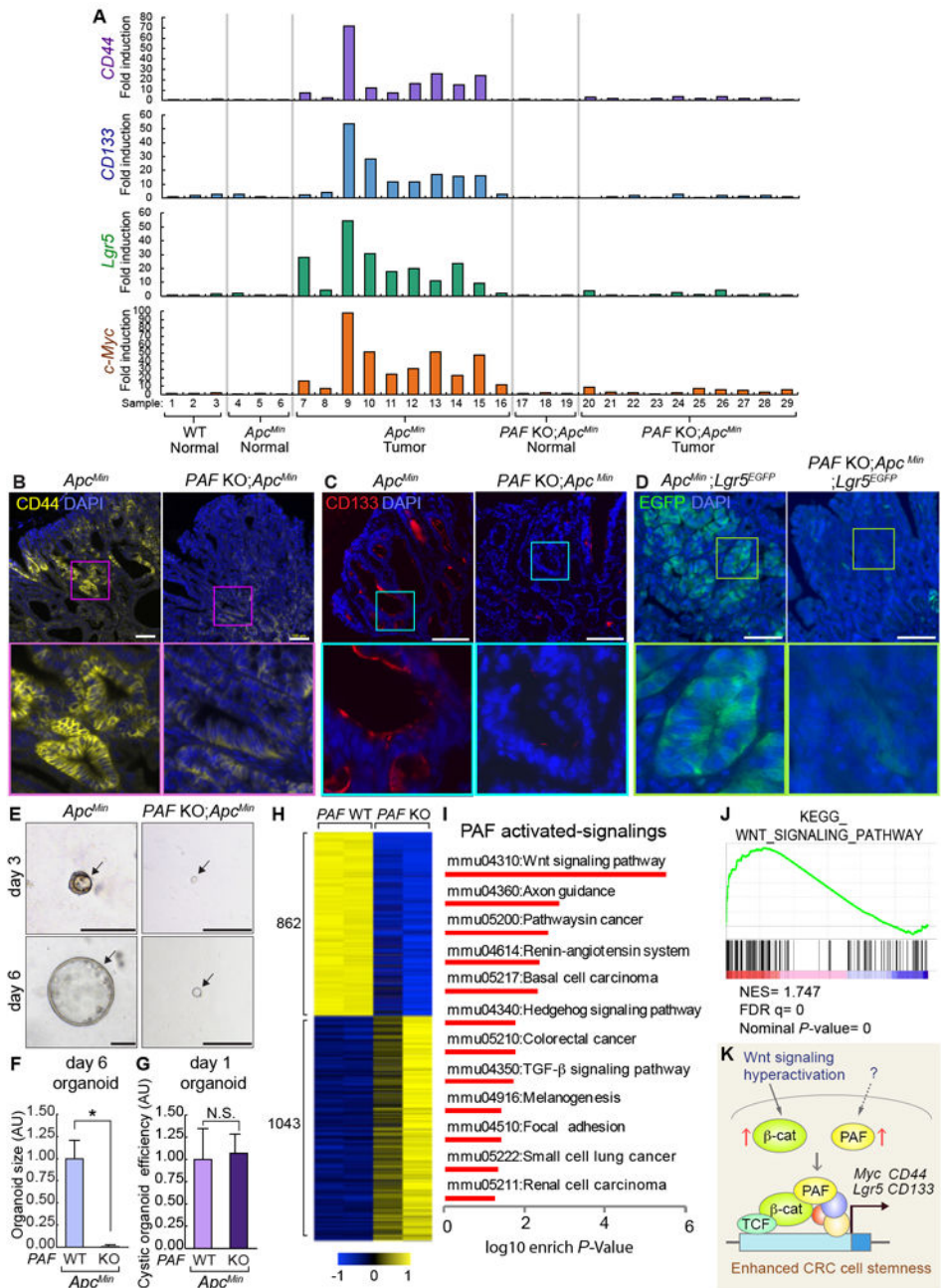


**Figure 7. Decreased CRC Cell Stemness by *PAF* KO**

(A) Gene expression analysis of *CD44*, *CD133*, *Lgr5*, and *c-Myc* in the normal intestine or adenomas from *Apc*<sup>Min/+</sup> and *PAF*KO;*Apc*<sup>Min/+</sup> (16 wk old). At least three individual samples from WT and normal region of *Apc*<sup>Min/+</sup> and *PAF*KO;*Apc*<sup>Min/+</sup> were used as the control.

(B, C) Downregulation of CD44 and CD133 expression in *Apc*<sup>Min</sup> tumors by *PAF*KO. IF staining for CD44 and CD133; 16 wk old. Scale bars=100µm.

(D) Downregulation of *Lgr5* in *Apc*<sup>Min</sup> tumors by *PAF*KO. IF for GFP (adenomas of *Apc*<sup>Min/+</sup>;*Lgr5*-EGFP and *PAF*KO;*Apc*<sup>Min/+</sup>;*Lgr5*-EGFP [16 wk old]). Scale bars=100 µm.

- (E) Reduced cystic organoid development by *PAFKO*. Representative images of organoids (day 5) derived from *Apc<sup>Min</sup>* and *PAFKO;Apc<sup>Min</sup>* adenomas
- (F, G) Quantification of organoid size (F) (N = 30 cystic organoids were analyzed); efficiency (G) (N = 5000 cells were analyzed for from three independent experiments). Scale bars=100 $\mu$ m. Asterisk: P<0.001.
- (H) Heatmap gene expression profile generated by significant differential expression (P<0.05) of *Apc<sup>Min/+</sup>* and *PAFKO;Apc<sup>Min</sup>* adenomas by RNA sequencing (N=2 per group).
- (I) Significantly PAF upregulated signaling pathways identified by GSEA analysis (KEGG) using RNA-seq result. P<0.05.
- (J) Gene set enrichment analysis (GSEA) for Wnt signaling pathway. NES: normalized enrichment score; FDR: False detection rate; P-value: Nominal P-value.
- (K) Illustration of the working model. During tumorigenesis, Wnt/ $\beta$ -catenin signaling is hyperactivated and PAF is upregulated. PAF and  $\beta$ -catenin transactivate *c-Myc* and CRC stemness-related genes (CD44, CD133, and Lgr5), which leads to the increase of CRC stemness.
- See also Figure S7, Tables S1 and S2.



## KEY RESOURCES TABLE

REAGENT or RESOURCE	SOURCE	IDENTIFIER
<b>Antibodies</b>		
Mouse anti-PAF (KIAA0101)	Santa Cruz Biotechnology	Cat# sc-390515
Mouse anti-PAF (KIAA0101)	Abcam	Cat# ab56773 RRID:AB_943922
Rabbit anti-PCNA	Cell Signaling Technology	Cat# 13110
Rabbit anti-Bmi1	Cell Signaling Technology	Cat# 6964S RRID:AB_10828713
Rabbit anti-RFP	Rockland	Cat# 600-401-379S RRID:AB_11182807
Rat anti-BrdU	Abcam	Cat# ab6326 RRID:AB_305426
Rabbit anti-Ki67	Abcam	Cat# ab16667 RRID:AB_302459
Mouse anti-E-Cadherin	BD Biosciences	Cat# 610182 RRID:AB_397581
Rabbit anti-Lysozyme	Abcam	Cat# ab108508 RRID:AB_10861277
Rabbit anti-Villin	Thermo Fisher Scientific	Cat# PA5-22072 RRID:AB_11155190
Rabbit anti-Chromogranin A	Abcam	Cat# ab15160 RRID:AB_301704
Rabbit anti-Phospho-Histone H2A.X (Ser139) (20E3)	Cell Signaling Technology	Cat# 9718S RRID:AB_2118009
Rabbit anti-Cleaved Caspase-3 (Asp175) (5A1E)	Cell Signaling Technology	Cat# 9664 RRID:AB_2070042
Rabbit anti- $\beta$ -Catenin (D10A8)	Cell Signaling Technology	Cat# 9587S RRID:AB_10695312
Rabbit anti-Non-phospho (Active) $\beta$ -Catenin (D13A1)	Cell Signaling Technology	Cat# 8814s RRID:AB_11127203
Rabbit anti-c-Myc (N262)	Santa Cruz Biotechnology	Cat# sc-764 RRID:AB_631276
Rabbit anti-Cyclin D1 (92G2)	Cell Signaling Technology	Cat# 2978P

REAGENT or RESOURCE	SOURCE	IDENTIFIER
		RRID:AB_10839128
<b>Rat anti-CD44</b>	BD Biosciences	Cat# 550538 RRID:AB_393732
<b>Rat anti-CD133</b>	eBioscience	Cat# 14-1331-82 RRID:AB_467471
<b>Mouse anti-P53 (Ab-1)</b>	Thermo Fisher Scientific	Cat# MS-104-P0 RRID:AB_64407
<b>Rabbit anti-P21 (M-19)</b>	Santa Cruz Biotechnology	Cat#sc-471 RRID:AB_632123
<b>Rabbit anti-Phospho-Chk1 (Ser345)</b>	Cell Signaling Technology	Cat#2341 RRID:AB_330023
<b>Mouse anti-ATM pS1981</b>	Rockland	Cat# 200-301-500 RRID:AB_828098
<b>Chemicals, Peptides, and Recombinant Proteins</b>		
<b>5-Bromo-2'-deoxyuridine</b>	Sigma	Cat# B5002
<b>Y-27632 dihydrochloride</b>	Sigma	Cat# Y0503
<b>Recombinant Mouse R-Spondin 1</b>	R&D Systems	Cat# 3474-RS-050
<b>Recombinant Murine Noggin</b>	Peptotech	Cat# 250-38
<b>Recombinant Murine EGF</b>	Peptotech	Cat# 315-09
<b>Jagged-1 peptide</b>	AnaSpec	AS-61298
<b>Critical Commercial Assays</b>		
<b>REPLI-g WTA Single Cell Kit</b>	Qiagen	Cat# 150063
<b>Experimental Models: Cell Lines</b>		
<b>FHC</b>	ATCC	CRL-1831 RRID:CVCL_3688
<b>HCT116</b>	ATCC	CCL-247 RRID:CVCL_0291
<b>SW620</b>	ATCC	CCL-227 RRID:CVCL_0547
<b>HT29</b>	ATCC	HTB-38 RRID:CVCL_0320
<b>Experimental Models: Organisms/Strains</b>		

REAGENT or RESOURCE	SOURCE	IDENTIFIER
<b>Mouse: <i>Lgr5-EGFP-IRES-creERT2</i> (B6.129P2-<i>Lgr5</i><sup>tm1(cre)ERT2/ChaJ</sup>)</b>	The Jackson Laboratory	JAX: 008875 RRID:IMSR_JAX:008875
<b>Mouse: <i>Apc</i><sup>Min/+</sup> (C57BL/6J-<i>Apc</i><sup>Min/J</sup>)</b>	The Jackson Laboratory	JAX: 002020 RRID:IMSR_JAX:002020
<b>Mouse: <i>TERT</i><sup>TCE/+</sup></b>	Jun et al., 2016	Jae-il Park, jaeil@mdanderson.org
<b>Mouse: <i>Bmi1</i><sup>EGFP</sup> (BKa.Cg-<i>Ptprcb Bmi1</i><sup>tm1llw</sup> <i>Thyl1a/J</i>)</b>	The Jackson Laboratory	JAX: 017351 RRID:IMSR_JAX:017351
<b>Mouse: C57BL/6J</b>	The Jackson Laboratory	JAX: 000664 RRID:IMSR_JAX:000664
<b>Recombinant DNA</b>		
<b><i>MSCV-c-Myc-IRES-RFP</i></b>	Kawauchi et al., 2012	Addgene #35395
<b>Sequence-Based Reagents</b>		
<b>Primers for qPCR and ChIP, see Table S3</b>	This paper	N/A
<b>Deposited Data</b>		
<b>RNA-seq data set</b>	This paper	GEO: GSE109209